

# Biological networks and GWAS: comparing and combining network methods to understand the genetics of familial breast cancer susceptibility in the GENESIS study

Héctor Climente-González<sup>1,2,3,4\*</sup>, Christine Lonjou<sup>1,2,3</sup>, Fabienne Lesueur<sup>1,2,3</sup>, Dominique Stoppa-Lyonnet<sup>5,6,7¤</sup>, Nadine Andrieu<sup>1,2,3</sup>, Chloé-Agathe Azencott<sup>3,1,2</sup>, with the GENESIS study group<sup>¶</sup>

**1** Institut Curie, PSL Research University, F-75005 Paris, France;

**2** INSERM, U900, F-75005 Paris, France;

**3** MINES ParisTech, PSL Research University, CBIO-Centre for Computational Biology, F-75006 Paris, France;

**4** RIKEN Center for Advanced Intelligence Project (AIP), Tokyo, Japan;

**5** Service de Génétique, Institut Curie, F-75005 Paris, France;

**6** INSERM, U830, F-75005 Paris, France;

**7** Université Paris Descartes.

¤For the GENESIS study group

¶Membership list can be found in the Acknowledgments section.

\* hector.climente(at)riken.jp

## Abstract

Network methods provide a comprehensive approach to uncovering the genetics of complex diseases and building hypotheses. They discover susceptibility genes by jointly consider the statistical association between genetic variation and a phenotype, measured in a genome-wide association study (GWAS), and the biological context of each gene, represented as a network. Hence, a network method could select a gene with a high P-value of association if it connects multiple low P-value genes in the network. In this work, we studied six network methods which identify subnetworks with high scores of GWAS association with a phenotype. This allows them to give more compelling results than standard SNP- and gene-level GWAS analyses, recovering causal subnetworks tightly related to cancer susceptibility. We applied them to GENESIS, a GWAS on French women with a family history of breast cancer and who tested negative for pathogenic variants in *BRCA1* and *BRCA2*. We critically compared these six methods, discussing the impact of their different mathematical frameworks, and the parameter choices. Additionally, we performed an in-depth benchmarking with respect to the size and predictive power of their solutions, as well as their stability and runtimes. Importantly, we found significant overlaps between the genes in five of the solution networks and the genes significantly associated in the largest GWAS on susceptibility to breast cancer. Since most of the methods produced reasonable solutions, we proposed to combine them into a consensus solution, containing the genes selected by at least two methods. This aggregation brought further insights. For instance, it contained *COPS5*, a gene related to multiple hallmarks of cancer, and 14 of its neighbors. The main drawback of network methods with regards to conventional  $\chi^2$ -based GWAS was instability i.e. network methods' outputs changed more in front of small perturbations in the input. To compensate for this instability, we proposed a stable consensus solution, formed by the most consistently selected genes in different subsamples of the data. This

stable consensus was composed of 68 genes, enriched in known breast cancer susceptibility genes (*BLM*, *CASP8*, *CASP10*, *DNAJC1*, *FGFR2*, *MRPS30*, and *SLC4A7*, Fisher's exact test P-value =  $3 \times 10^{-4}$ ) and occupying more central positions in the network than most genes. The network was organized around *CUL3*, which encodes a ubiquitin ligase related protein that regulates the protein levels of several genes involved in cancer progression. In conclusion, we showed how network address limitations of GWAS, namely their lack of statistical power and the difficulty of their interpretation. Project-agnostic implementations of each of the network methods are available at <https://github.com/hclimente/gwas-tools> to facilitate their application to other GWAS datasets.

## Author summary

In genome-wide association studies (GWAS), thousands of genomes are scanned to identify variants associated with a complex trait. Over the last 15 years, GWAS have advanced our understanding of the genetics of complex diseases, and in particular of hereditary cancers. Yet, they have led to an apparent paradox: the more we perform such studies, the more it seems that the entire genome is involved in every disease. The omnigenic model offers an appealing explanation: only a limited number of core genes are directly involved in the disease; but gene functions are deeply interrelated so that many other genes can alter the function of the core genes. These interrelations are often modeled as networks, and multiple algorithms have been proposed to use these networks to identify the subset of core genes involved in a specific trait. In this study, we characterize six such network methods on GENESIS, a GWAS dataset for familial breast cancer in the French population. Combining these approaches allows us to identify potentially novel breast cancer susceptibility genes, and provides a mechanistic explanation for their role in the development of the disease. We provide ready-to-use implementations of all the examined methods.

## 1 Introduction

In human health, genome-wide association studies (GWAS) aim at quantifying how single-nucleotide polymorphisms (SNPs) predispose to complex diseases, like diabetes or some forms of cancer [1]. To that end, in a typical GWAS thousands of unrelated samples are genotyped: the cases, suffering from the disease of interest, and the controls, taken from the general population. Then, a statistical test of association (e.g. based on logistic regression) is conducted between each individual SNP and the phenotype. Those SNPs with a P-value lower than a conservative Bonferroni threshold are candidates to further studies in an independent cohort. Once the risk SNPs have been discovered, they can be used for risk assessment, and to deepen our understanding of the disease.

GWAS have successfully identified thousands of variants underlying many common diseases [2]. However, this experimental setting also presents intrinsic challenges. Some of them stem from the high dimensionality of the problem, as every GWAS to date studies more variants than samples are genotyped. This limits the statistical power of the experiment, as only variants with larger effects can be detected [3]. This is particularly problematic since the prevailing view is that most genetic architectures involve many variants with small effects [3]. Additionally, to avoid false positives, a conservative multiple test correction is applied, typically the previously mentioned Bonferroni correction. However, Bonferroni correction is overly conservative when the statistical tests are correlated, as it is the case in GWAS [4]. Another open issue is the interpretation of the results, as the functional consequences of most common variants

are unknown. On top of that, recent large-sampled studies suggest that numerous loci spread all along the genome contribute to a degree to any complex trait, in accordance with the infinitesimal model [5]. The recently proposed omnigenic model [6] offers an explanation: genes are strongly inter-related and influence each other's function, which allows alterations in most genes to impact the subset of "core" genes directly involved in the disease's mechanism. Hence, a comprehensive statistical framework which includes the structure of biological data might help alleviate the aforementioned issues.

For this reason, many authors turn to network biology to handle the complex interplay of biomolecules that lead to disease [7]. As its name suggests, network biology models biology as a network, where the biomolecules under study, often genes, are nodes, and selected functional relationships are edges that link them. These relationships come from evidence that the genes jointly contribute to a biological function; for instance, their expression is correlated, or their products establish a protein-protein interaction. Under this view, complex diseases are not the consequence of a single altered gene, but of the interaction of multiple interdependent molecules [8]. In fact, an examination of biological networks shows that disease genes have differential properties [8,9]: they tend to occupy central positions in the network, interconnecting different modules TODO. Therefore, studying the neighborhood of disease-associated genes is effective at identifying new ones that are involved in the same biological functions [10].

Network-based discovery methods exploit the differential properties described above to identify disease genes on GWAS data [11]. In essence, each gene is assigned a score of association with the disease, computed from the GWAS data, and biological relationships, given by a network built on prior knowledge. Then, the problem becomes finding a functionally-related set of highly-scoring genes. Multiple solutions have been proposed to this problem, often stemming from different mathematical frameworks and considerations of what the optimal solution looks like. For example, some methods restrict the problem to specific types of subnetworks. Such is the case of LEAN [12], which focuses on "star" subnetworks, i.e. instances were both a gene and its direct interactors are associated with the disease. Other algorithms, like dmGWAS [13] and heinz [14], do not impose such strong constraints, and search for subnetworks interconnecting genes with high association scores. However, they differ in their tolerance to the inclusion of low-scoring nodes, and the topology of the solution. Lastly, other methods also consider the topology of the network, favoring groups of nodes that are not only high-scoring, but also densely interconnected; such is the case of HotNet2 [15], SConES [16], and SigMod [17].

In this work, we analyze the application of these six network methods on GWAS data. They use different interpretations of the omnigenic model, and provide a representative view of the field. We worked on the GENESIS dataset [18], a study on familial breast cancer conducted in the French population. After a classical GWAS approach, we use these network methods to recover additional breast cancer susceptibility genes. Lastly, we carry out a comparison of the solutions obtained by the different methods, and aggregate them to obtain a consensus solution of predisposition to familial breast cancer.

## 2 Results

### 2.1 Conventional SNP- and gene-based analyses confirm that *FGFR2* locus is associated with familial breast cancer

We conducted association analyses in the GENESIS dataset (Section 4.1) at both SNP and gene levels (Section 4.2). Two genomic regions had a P-value lower than the Bonferroni threshold on chromosomes 10 and 16 (S2 FigA). The former overlaps with

gene *FGFR2*; the latter with *CASC16* the protein-coding gene *TOX3*. Variants in both *FGFR2* and *TOX3* have been repeatedly associated with breast cancer susceptibility in other case-control studies [19], *BRCA1* and *BRCA2* carrier studies [20], and in hereditary breast and ovarian cancer families negative for mutations in *BRCA1* and *BRCA2* [21]. In GENESIS only *FGFR2* was significantly associated with breast cancer at the gene-level (S2 FigB).

Closer examination reveals two other regions (3p24 and 8q24) having low, albeit not genome-wide significant, P-values. Both of them have been associated to breast cancer susceptibility in the past [22, 23]. We applied an L1-penalized logistic regression using all the GENESIS genotypes as input, and the phenotype (cancer/healthy) as outcome (Section 4.5.2). The algorithm selected 100 SNPs, both from all aforementioned regions and new ones (S2 FigC). Yet, it is unclear why those SNPs were selected, as emphasized by the high P-value of some of them, which further complicates the biological interpretation. Moreover, and in opposition to what would be expected under the omnigenic model, the genes to which these SNPs map to (Section 4.3.5) are not interconnected in the protein-protein interaction network (PPIN, Section 4.3.2). Moreover, the classification performance of the model is low (sensitivity = 55%, specificity = 55%, Section 4.5). Together, these issues motivate exploring network methods, which consider not only statistical association, but also the location of each gene in a PPIN to find susceptibility genes.

## 2.2 Network methods successfully identify genes associated with breast cancer

We applied six network methods to the GENESIS dataset (Section 4.3.3). As none of the networks examined by LEAN was significant (Benjamini-Hochberg [BH] correction adjusted P-value < 0.05), we obtained six solutions (Fig 1): one for each of the remaining four gene-based methods, one for SConES GI (which works at the SNP level), and the consensus.

These solutions differ in many aspects, making it hard to draw joint conclusions. For starters, the overlap between the genes featured in each solution is quite small (Fig 1A). However, the methods tend to agree on the genes with the strongest signal: genes selected by more methods tended to have lower P-value of association (Fig 1B).

Another prominent difference is the solution size: the largest solution, produced by HotNet2, contains 440 genes, while heinz's contains only 4 genes. While SConES GI did not recover any protein coding gene, working with SNP networks rather than gene networks allowed it to retrieve four subnetworks in intergenic regions, and another one overlapping an RNA gene (*RNU6-420P*).

The topologies of the six solutions differ as well (Fig 1C), as measured by the median centrality and the number of connected components (Table 1). Only two methods yield more than one connected component: SConES, as described above, and HotNet2. HotNet2 produced 135 subnetworks, 115 of which have fewer than five genes. The second largest subnetwork (13 nodes) contains the two breast cancer susceptibility genes *CASP8* and *BLM*.

Lastly, a pathway enrichment analysis (Section 4.4) also showed similarities and differences between the solutions of the different methods. It linked different parts of SigMod's solution to four processes (S3 Table): protein translation (including mitochondrial), mRNA splicing, protein misfolding, and keratinization (BH adjusted P-values < 0.03). Interestingly, the dmGWAS solution (S4 Table) is also related to protein misfolding (*attenuation phase*, BH adjusted P-value = 0.01). However, it additionally includes submodules of proteins related to mitosis, DNA damage, and regulation of TP53 (BH adjusted P-values < 0.05), which match previously known

mechanisms of breast cancer susceptibility [24]. As with SigMod, the genes in HotNet2's solution (S5 Table) are involved in mitochondrial translation (BH adjusted P-value =  $1.87 \times 10^{-4}$ ), but also in glycogen metabolism and transcription of nuclear receptors (BH adjusted P-value < 0.04). 136  
137  
138  
139

**Table 1.** Summary statistics on the solutions of multiple network methods on the PPIN. The first row contains the summary statistics on the whole PPIN.

Network	# genes	# edges	# components	Betweenness	$\hat{P}_{\text{gene}}$	# genes in consensus
HINT HT	13 619	142 541	15	16 706	0.46	93/93
dmGWAS	194	450	1	49 115	0.19	55/93
heinz	4	3	1	113 633	0.001	4/93
HotNet2	440	374	130	7 739	0.048	63/93
LEAN	0	0	0	-	-	0/93
SConES GI	0 (1)	0	0	-	-	0/93
SigMod	142	249	11	92 603	0.008	84/93
Consensus	93	186	21	50 737	0.006	93/93
Stable consensus	68	49	32	94 854	0.005	43/93

**# genes:** number of genes selected out of those that are part of the PPIN; for SConES GI the total number of genes, including RNA genes, was added in parentheses. **# components :** number of connected components. **Betweenness:** mean betweenness of the selected genes in the PPIN.  **$\hat{P}_{\text{gene}}$ :** median VEGAS2 P-value of the selected genes. **# genes in consensus:** Number of genes in common between the method's solution, and the 93 genes in the consensus solution. 140  
141  
142  
143  
144  
145  
146  
147

Despite their differences, there are additional common themes. All obtained solutions have lower association P-values than the whole PPIN (median VEGAS2 P-value  $\ll 0.46$ , Table 1), despite containing genes with higher P-values as well (Fig 1D). This illustrates the trade-off between controlling for type I error and biological relevance. However, there are nuances between solutions in this regard: heinz strongly favors genes with lower P-values, while dmGWAS is less conservative (median VEGAS2 P-values 0.0012 and 0.19, respectively); SConES tends to select whole LD-blocks; and HotNet2 and SigMod are less likely to select low scoring genes. 148  
149  
150  
151  
152  
153  
154  
155  
156  
157  
158

Additionally, the solutions presented other desirable properties. First, five of them were enriched in known breast cancer susceptibility genes (consensus, dmGWAS, heinz, HotNet2, and SigMod, Fisher's exact test one-sided P-value  $< 0.03$ ). Second, the genes in four solutions displayed on average a higher betweenness centrality than the rest of the genes, a difference that is significant in four solutions (consensus, dmGWAS, HotNet2, and SigMod, Wilcoxon rank-sum test P-value  $< 1.4 \times 10^{-21}$ ). This agrees with the notion that disease genes are more central than other non-essential genes [9], an observation that holds in breast cancer (one-tailed Wilcoxon rank-sum test P-value =  $2.64 \times 10^{-5}$  when comparing the betweenness of known susceptibility genes versus the rest). Interestingly, SConES selected SNPs that are also more central than the average SNP (S1 Table), suggesting that causal SNPs are also more central than non-associated SNPs. 159  
160  
161  
162  
163  
164  
165  
166  
167

### 2.3 A case study: the consensus solution

Despite their shared properties, the differences between the solutions of the different methods suggest that each of them captures different aspects of cancer susceptibility. Indeed, out of the 668 genes that are selected by at least one method, only 93 are selected by at least two, 20 by three, and none by four or more. Encouragingly, the more methods selected a gene, the higher its association score to the phenotype (Fig 1B), a relationship that plateaus at 2. Hence, to leverage on their strengths and compensate their respective weaknesses, we built a consensus solution that captures the genes shared among at least two solutions (Section 4.3.3). This solution (Fig 2) contains 93 genes and 168  
169  
170  
171  
172  
173  
174  
175  
176  
177  
178  
179  
180  
181  
182  
183  
184  
185  
186  
187  
188  
189  
190  
191  
192  
193  
194  
195  
196  
197  
198  
199  
200  
201  
202  
203  
204  
205  
206  
207  
208  
209  
210  
211  
212  
213  
214  
215  
216  
217  
218  
219  
220  
221  
222  
223  
224  
225  
226  
227  
228  
229  
230  
231  
232  
233  
234  
235  
236  
237  
238  
239  
240  
241  
242  
243  
244  
245  
246  
247  
248  
249  
250  
251  
252  
253  
254  
255  
256  
257  
258  
259  
260  
261  
262  
263  
264  
265  
266  
267  
268  
269  
270  
271  
272  
273  
274  
275  
276  
277  
278  
279  
280  
281  
282  
283  
284  
285  
286  
287  
288  
289  
290  
291  
292  
293  
294  
295  
296  
297  
298  
299  
300  
301  
302  
303  
304  
305  
306  
307  
308  
309  
310  
311  
312  
313  
314  
315  
316  
317  
318  
319  
320  
321  
322  
323  
324  
325  
326  
327  
328  
329  
330  
331  
332  
333  
334  
335  
336  
337  
338  
339  
340  
341  
342  
343  
344  
345  
346  
347  
348  
349  
350  
351  
352  
353  
354  
355  
356  
357  
358  
359  
360  
361  
362  
363  
364  
365  
366  
367  
368  
369  
370  
371  
372  
373  
374  
375  
376  
377  
378  
379  
380  
381  
382  
383  
384  
385  
386  
387  
388  
389  
390  
391  
392  
393  
394  
395  
396  
397  
398  
399  
400  
401  
402  
403  
404  
405  
406  
407  
408  
409  
410  
411  
412  
413  
414  
415  
416  
417  
418  
419  
420  
421  
422  
423  
424  
425  
426  
427  
428  
429  
430  
431  
432  
433  
434  
435  
436  
437  
438  
439  
440  
441  
442  
443  
444  
445  
446  
447  
448  
449  
450  
451  
452  
453  
454  
455  
456  
457  
458  
459  
460  
461  
462  
463  
464  
465  
466  
467  
468  
469  
470  
471  
472  
473  
474  
475  
476  
477  
478  
479  
480  
481  
482  
483  
484  
485  
486  
487  
488  
489  
490  
491  
492  
493  
494  
495  
496  
497  
498  
499  
500  
501  
502  
503  
504  
505  
506  
507  
508  
509  
510  
511  
512  
513  
514  
515  
516  
517  
518  
519  
520  
521  
522  
523  
524  
525  
526  
527  
528  
529  
530  
531  
532  
533  
534  
535  
536  
537  
538  
539  
540  
541  
542  
543  
544  
545  
546  
547  
548  
549  
550  
551  
552  
553  
554  
555  
556  
557  
558  
559  
560  
561  
562  
563  
564  
565  
566  
567  
568  
569  
570  
571  
572  
573  
574  
575  
576  
577  
578  
579  
580  
581  
582  
583  
584  
585  
586  
587  
588  
589  
590  
591  
592  
593  
594  
595  
596  
597  
598  
599  
600  
601  
602  
603  
604  
605  
606  
607  
608  
609  
610  
611  
612  
613  
614  
615  
616  
617  
618  
619  
620  
621  
622  
623  
624  
625  
626  
627  
628  
629  
630  
631  
632  
633  
634  
635  
636  
637  
638  
639  
640  
641  
642  
643  
644  
645  
646  
647  
648  
649  
650  
651  
652  
653  
654  
655  
656  
657  
658  
659  
660  
661  
662  
663  
664  
665  
666  
667  
668  
669  
670  
671  
672  
673  
674  
675  
676  
677  
678  
679  
680  
681  
682  
683  
684  
685  
686  
687  
688  
689  
690  
691  
692  
693  
694  
695  
696  
697  
698  
699  
700  
701  
702  
703  
704  
705  
706  
707  
708  
709  
710  
711  
712  
713  
714  
715  
716  
717  
718  
719  
720  
721  
722  
723  
724  
725  
726  
727  
728  
729  
730  
731  
732  
733  
734  
735  
736  
737  
738  
739  
740  
741  
742  
743  
744  
745  
746  
747  
748  
749  
750  
751  
752  
753  
754  
755  
756  
757  
758  
759  
750  
751  
752  
753  
754  
755  
756  
757  
758  
759  
760  
761  
762  
763  
764  
765  
766  
767  
768  
769  
770  
771  
772  
773  
774  
775  
776  
777  
778  
779  
770  
771  
772  
773  
774  
775  
776  
777  
778  
779  
780  
781  
782  
783  
784  
785  
786  
787  
788  
789  
780  
781  
782  
783  
784  
785  
786  
787  
788  
789  
790  
791  
792  
793  
794  
795  
796  
797  
798  
799  
790  
791  
792  
793  
794  
795  
796  
797  
798  
799  
800  
801  
802  
803  
804  
805  
806  
807  
808  
809  
800  
801  
802  
803  
804  
805  
806  
807  
808  
809  
810  
811  
812  
813  
814  
815  
816  
817  
818  
819  
810  
811  
812  
813  
814  
815  
816  
817  
818  
819  
820  
821  
822  
823  
824  
825  
826  
827  
828  
829  
820  
821  
822  
823  
824  
825  
826  
827  
828  
829  
830  
831  
832  
833  
834  
835  
836  
837  
838  
839  
830  
831  
832  
833  
834  
835  
836  
837  
838  
839  
840  
841  
842  
843  
844  
845  
846  
847  
848  
849  
840  
841  
842  
843  
844  
845  
846  
847  
848  
849  
850  
851  
852  
853  
854  
855  
856  
857  
858  
859  
850  
851  
852  
853  
854  
855  
856  
857  
858  
859  
860  
861  
862  
863  
864  
865  
866  
867  
868  
869  
860  
861  
862  
863  
864  
865  
866  
867  
868  
869  
870  
871  
872  
873  
874  
875  
876  
877  
878  
879  
870  
871  
872  
873  
874  
875  
876  
877  
878  
879  
880  
881  
882  
883  
884  
885  
886  
887  
888  
889  
880  
881  
882  
883  
884  
885  
886  
887  
888  
889  
890  
891  
892  
893  
894  
895  
896  
897  
898  
899  
890  
891  
892  
893  
894  
895  
896  
897  
898  
899  
900  
901  
902  
903  
904  
905  
906  
907  
908  
909  
900  
901  
902  
903  
904  
905  
906  
907  
908  
909  
910  
911  
912  
913  
914  
915  
916  
917  
918  
919  
910  
911  
912  
913  
914  
915  
916  
917  
918  
919  
920  
921  
922  
923  
924  
925  
926  
927  
928  
929  
920  
921  
922  
923  
924  
925  
926  
927  
928  
929  
930  
931  
932  
933  
934  
935  
936  
937  
938  
939  
930  
931  
932  
933  
934  
935  
936  
937  
938  
939  
940  
941  
942  
943  
944  
945  
946  
947  
948  
949  
940  
941  
942  
943  
944  
945  
946  
947  
948  
949  
950  
951  
952  
953  
954  
955  
956  
957  
958  
959  
950  
951  
952  
953  
954  
955  
956  
957  
958  
959  
960  
961  
962  
963  
964  
965  
966  
967  
968  
969  
960  
961  
962  
963  
964  
965  
966  
967  
968  
969  
970  
971  
972  
973  
974  
975  
976  
977  
978  
979  
970  
971  
972  
973  
974  
975  
976  
977  
978  
979  
980  
981  
982  
983  
984  
985  
986  
987  
988  
989  
980  
981  
982  
983  
984  
985  
986  
987  
988  
989  
990  
991  
992  
993  
994  
995  
996  
997  
998  
999  
990  
991  
992  
993  
994  
995  
996  
997  
998  
999  
1000  
1001  
1002  
1003  
1004  
1005  
1006  
1007  
1008  
1009  
1000  
1001  
1002  
1003  
1004  
1005  
1006  
1007  
1008  
1009  
1010  
1011  
1012  
1013  
1014  
1015  
1016  
1017  
1018  
1019  
1010  
1011  
1012  
1013  
1014  
1015  
1016  
1017  
1018  
1019  
1020  
1021  
1022  
1023  
1024  
1025  
1026  
1027  
1028  
1029  
1020  
1021  
1022  
1023  
1024  
1025  
1026  
1027  
1028  
1029  
1030  
1031  
1032  
1033  
1034  
1035  
1036  
1037  
1038  
1039  
1030  
1031  
1032  
1033  
1034  
1035  
1036  
1037  
1038  
1039  
1040  
1041  
1042  
1043  
1044  
1045  
1046  
1047  
1048  
1049  
1040  
1041  
1042  
1043  
1044  
1045  
1046  
1047  
1048  
1049  
1050  
1051  
1052  
1053  
1054  
1055  
1056  
1057  
1058  
1059  
1050  
1051  
1052  
1053  
1054  
1055  
1056  
1057  
1058  
1059  
1060  
1061  
1062  
1063  
1064  
1065  
1066  
1067  
1068  
1069  
1060  
1061  
1062  
1063  
1064  
1065  
1066  
1067  
1068  
1069  
1070  
1071  
1072  
1073  
1074  
1075  
1076  
1077  
1078  
1079  
1070  
1071  
1072  
1073  
1074  
1075  
1076  
1077  
1078  
1079  
1080  
1081  
1082  
1083  
1084  
1085  
1086  
1087  
1088  
1089  
1080  
1081  
1082  
1083  
1084  
1085  
1086  
1087  
1088  
1089  
1090  
1091  
1092  
1093  
1094  
1095  
1096  
1097  
1098  
1099  
1090  
1091  
1092  
1093  
1094  
1095  
1096  
1097  
1098  
1099  
1100  
1101  
1102  
1103  
1104  
1105  
1106  
1107  
1108  
1109  
1100  
1101  
1102  
1103  
1104  
1105  
1106  
1107  
1108  
1109  
1110  
1111  
1112  
1113  
1114  
1115  
1116  
1117  
1118  
1119  
1110  
1111  
1112  
1113  
1114  
1115  
1116  
1117  
1118  
1119  
1120  
1121  
1122  
1123  
1124  
1125  
1126  
1127  
1128  
1129  
1120  
1121  
1122  
1123  
1124  
1125  
1126  
1127  
1128  
1129  
1130  
1131  
1132  
1133  
1134  
1135  
1136  
1137  
1138  
1139  
1130  
1131  
1132  
1133  
1134  
1135  
1136  
1137  
1138  
1139  
1140  
1141  
1142  
1143  
1144  
1145  
1146  
1147  
1148  
1149  
1140  
1141  
1142  
1143  
1144  
1145  
1146  
1147  
1148  
1149  
1150  
1151  
1152  
1153  
1154  
1155  
1156  
1157  
1158  
1159  
1150  
1151  
1152  
1153  
1154  
1155  
1156  
1157  
1158  
1159  
1160  
1161  
1162  
1163  
1164  
1165  
1166  
1167  
1168  
1169  
1160  
1161  
1162  
1163  
1164  
1165  
1166  
1167  
1168  
1169  
1170  
1171  
1172  
1173  
1174  
1175  
1176  
1177  
1178  
1179  
1170  
1171  
1172  
1173  
1174  
1175  
1176  
1177  
1178  
1179  
1180  
1181  
1182  
1183  
1184  
1185  
1186  
1187  
1188  
1189  
1180  
1181  
1182  
1183  
1184  
1185  
1186  
1187  
1188  
1189  
1190  
1191  
1192  
1193  
1194  
1195  
1196  
1197  
1198  
1199  
1190  
1191  
1192  
1193  
1194  
1195  
1196  
1197  
1198  
1199  
1200  
1201  
1202  
1203  
1204  
1205  
1206  
1207  
1208  
1209  
1200  
1201  
1202  
1203  
1204  
1205  
1206  
1207  
1208  
1209  
1210  
1211  
1212  
1213  
1214  
1215  
1216  
1217  
1218  
1219  
1210  
1211  
1212  
1213  
1214  
1215  
1216  
1217  
1218  
1219  
1220  
1221  
1222  
1223  
1224  
1225  
1226  
1227  
1228  
1229  
1220  
1221  
1222  
1223  
1224  
1225  
1226  
1227  
1228  
1229  
1230  
1231  
1232  
1233  
1234  
1235  
1236  
1237  
1238  
1239  
1230  
1231  
1232  
1233  
1234  
1235  
1236  
1237  
1238  
1239  
1240  
1241  
1242  
1243  
1244  
1245  
1246  
1247  
1248  
1249  
1240  
1241  
1242  
1243  
1244  
1245  
1246  
1247  
1248  
1249  
1250  
1251  
1252  
1253  
1254  
1255  
1256  
1257  
1258  
1259  
1250  
1251  
1252  
1253  
1254  
1255  
1256  
1257  
1258  
1259  
1260  
1261  
1262  
1263  
1264  
1265  
1266  
1267  
1268  
1269  
1260  
1261  
1262  
1263  
1264  
1265  
1266  
1267  
1268  
1269  
1270  
1271  
1272  
1273  
1274  
1275  
1276  
1277  
1278  
1279  
1270  
1271  
1272  
1273  
1274  
1275  
1276  
1277  
1278  
1279  
1280  
1281  
1282  
1283  
1284  
1285  
1286  
1287  
1288  
1289  
1280  
1281  
1282  
1283  
1284  
1285  
1286  
1287  
1288  
1289  
1290  
1291  
1292  
1293  
1294  
1295  
1296  
1297  
1298  
1299  
1290  
1291  
1292  
1293  
1294  
1295  
1296  
1297  
1298  
1299  
1300  
1301  
1302  
1303  
1304  
1305  
1306  
1307  
1308  
1309  
1300  
1301  
1302  
1303  
1304  
1305  
1306  
1307  
1308  
1309  
1310  
1311  
1312  
1313  
1314  
1315  
1316  
1317  
1318  
1319  
1310  
1311  
1312  
1313  
1314  
1315  
1316  
1317  
1318  
1319  
1320  
1321  
1322  
1323  
1324  
1325  
1326  
13

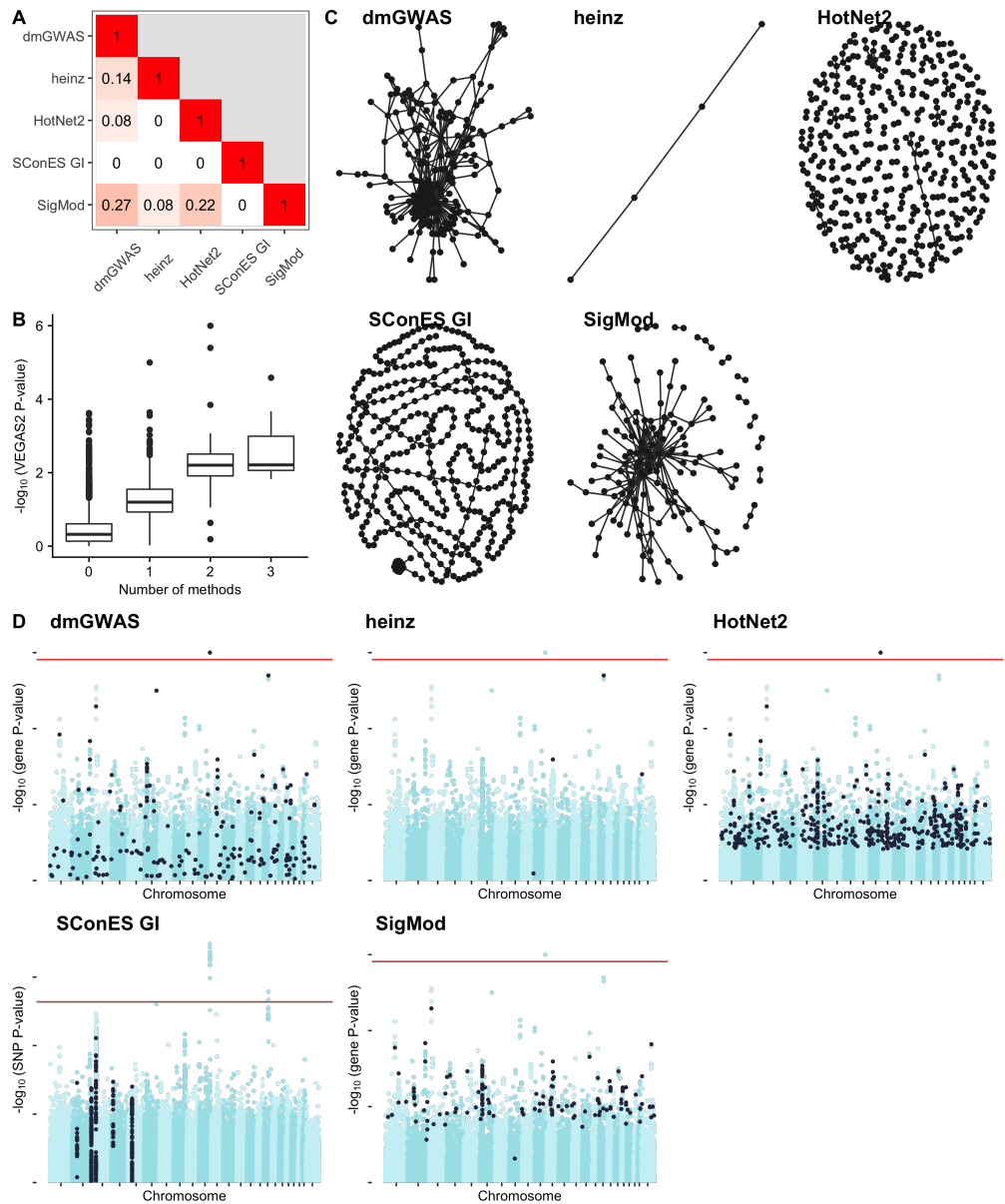


**Fig 1. Overview of the solutions produced by the different network methods (Section 4.3.3) on the GENESIS dataset.** As LEAN did not produce any significant solution (BH adjusted P-value < 0.05), it was excluded. Unless indicated otherwise, results refer to genes, except for SConES GI which are at the SNP-level. **(A)** Overlap between the genes selected by each of the methods, measured by Pearson correlation between indicator vectors. **(B)** VEGAS2 P-values of the genes in the PPIN not selected by any network method (12 213), and of those selected by 1 (575), 2 (73), or 3 (20) methods. **(C)** Solution networks produced by the different methods. **(D)** Manhattan plots of SNPs/genes; in black, the method's solution. The Bonferroni threshold is indicated by a red line ( $2.54 \times 10^{-7}$  for SNPs,  $1.53 \times 10^{-6}$  for genes).

exhibits the aforementioned properties of the individual solutions: enrichment in breast cancer susceptibility genes and higher betweenness centrality than the rest of the genes.

A pathway enrichment analysis of the genes in the consensus solution also shows

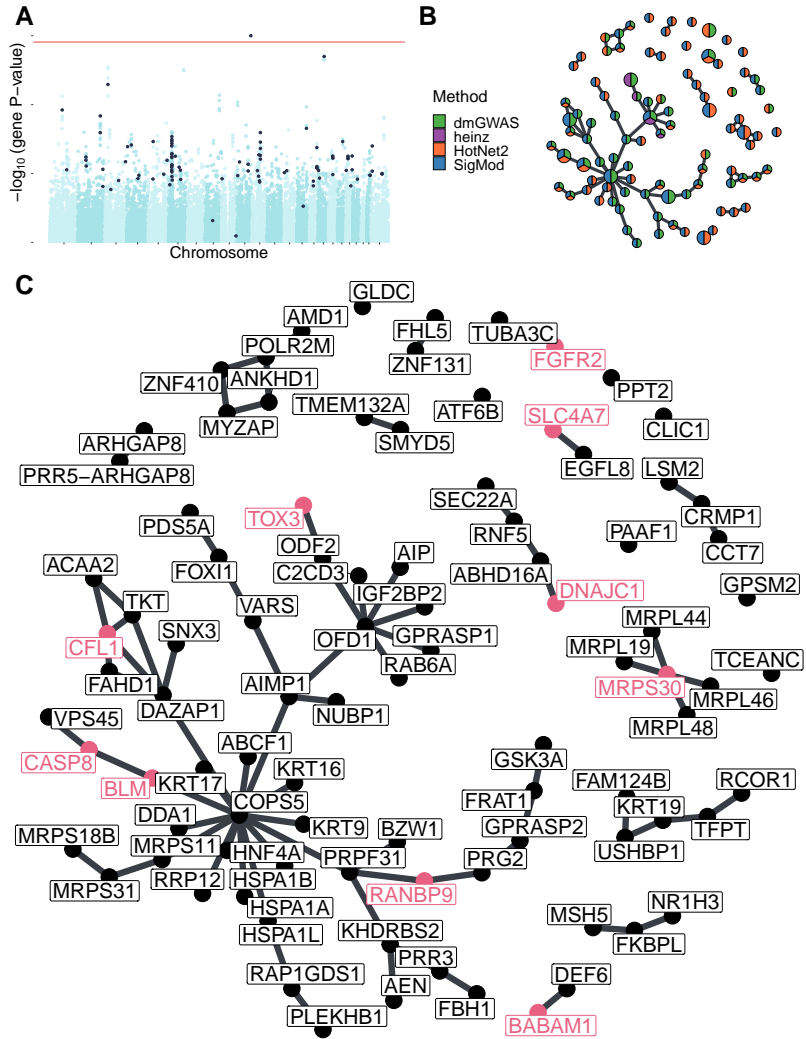


**Fig 2. Consensus solution on GENESIS (Section 4.3.3) .** **A** Manhattan plots of genes; in black, the ones in the consensus solution. The Bonferroni threshold is indicated by a red line ( $1.53 \times 10^{-6}$  for genes). **B** Consensus network. Each gene is represented by a pie chart, which shows the methods that selected it. We enlarged the two most central genes (*COPS5* and *OFD1*) and those genes that are known breast cancer susceptibility genes and/or significantly associated with breast cancer susceptibility in the BCAC dataset (Section 4.5.3). **C** The nodes are in the same disposition as in panel B, but every gene name is indicated. We colored in pink the names of genes that are known breast cancer susceptibility genes and/or significantly associated with breast cancer susceptibility in the BCAC dataset

similar pathways as the individual solutions (S6 Table). We found two involved mechanisms: *mitochondrial translation* and *attenuation phase*. The former is supported by genes like *MRPS30* (VEGAS2 P-value = 0.001), which encode a mitochondrial ribosomal protein and was also linked to breast cancer susceptibility [25]. Interestingly, increased mitochondrial translation has been found in cancer cells [26], and its inhibition proposed as a therapeutic target. With regards to the attenuation phase of heat shock response, it involves three Hsp70 chaperones: *HSPA1A*, *HSPA1B*, and

HSPA1L. The genes encoding these proteins are all near each other at 6p21, in the region known as HLA. In fact, out of the 22 SNPs that map to any of these three genes, 9 map to all of them, and 4 to two, making it hard to disentangle their effects. *HSPA1A* was the most strongly associated gene (VEGAS2 P-value =  $8.37 \times 10^{-4}$ ).  
178  
179  
180  
181

Topologically, the consensus consists of a connected component composed of 49 genes, and multiple smaller subnetworks. Among the latter, 19 genes are in subnetworks containing a single gene or two connected nodes, implying that they do not have a consistently altered neighborhood, but are strongly associated themselves and hence picked by at least two methods. The large connected component contains genes that are highly central in the PPIN, a property which is weakly anti-correlated with the P-value of association to the disease (Pearson correlation coefficient = -0.26, S4 Fig). This suggests that these genes were selected because they were on the shortest path between another two highly associated genes. In view of this, we hypothesize that highly central genes might contribute to the heritability through alterations of their neighborhood, consistently with the omnigenic model of disease [6]. For instance, the most central node in the consensus solution is COPS5, a component of the COP9 signalosome which regulates multiple signaling pathways. *COPS5* is related to multiple hallmarks of cancer and is overexpressed in multiple tumors, including breast and ovarian cancer [27]. Despite its lack of association in GENESIS or BCAC (VEGAS2 P-value of 0.22 and 0.14 respectively), its neighbors in the consensus solution have consistently low P-values (median VEGAS2 P-value = 0.006).  
182  
183  
184  
185  
186  
187  
188  
189  
190  
191  
192  
193  
194  
195  
196  
197  
198

## 2.4 Network methods boost discovery

We compared the results obtained with different network methods to the European sample of the Breast Cancer Association Consortium (BCAC) [19], the largest GWAS to date on breast cancer (Section 4.5.3). Although BCAC case-control studies do not necessarily target cases with a familial history of breast cancer, this comparison is pertinent since we expect a shared genetic architecture at the gene level, at which most network methods operate. This shared genetic architecture, together with BCAC's scale (90 times more samples than GENESIS) provides a reasonable counterfactual of what we would expect if GENESIS had a larger sample size. We computed a gene association score on BCAC (Section 4.5.3). The solutions provided by the different network methods overlap significantly with BCAC findings (Fisher's exact test P-value < 0.019). The gene-based methods achieve comparable precision (2%-25%) and recall (1.3-12.1%) at recovering BCAC-significant genes (S5 FigA). Interestingly, while SConES GI, at the SNP-level, achieves a similar recall (8.6%), it shows a much higher precision (47.3%).  
199  
200  
201  
202  
203  
204  
205  
206  
207  
208  
209  
210  
211  
212

## 2.5 Network methods share limitations

We compared the six network methods in a 5-fold subsampling setting (Section 4.5). This allowed us to measure five properties (Fig 3): size of the solution; sensitivity and specificity of an L1-penalized logistic regression classifier on the selected SNPs; stability; and computational runtime. The solution size varies greatly between the different methods (Fig 3A). Heinz produced the smallest solutions, with an average of 182 selected SNPs (Section 4.3.5). The largest solutions came from SConES GI (6 256.6 SNPs), and dmGWAS (4 255.0 SNPs). LEAN did not produce any solution in any of the subsamples. Using different combinations of parameters (Section 4.3.4), we computed how good each of the methods was at recovering the results of a conventional GWAS on BCAC (Section 4.5.3, Fig 3B). SConES exhibits the largest area under the curve, since, when  $\lambda = 0$  (network topology is disregarded), it is equivalent to a Bonferroni correction. Between the remaining network methods, they have similar areas under the curve, with heinz being the one with the largest area.  
213  
214  
215  
216  
217  
218  
219  
220  
221  
222  
223  
224  
225  
226

To determine whether the selected SNPs could be used for patient classification, we  
227  
computed the performance of the classifier on the *test dataset* (S5 FigB). The different  
228  
classifiers displayed similarly poor sensitivities and specificities, all in the 0.52 – 0.56  
229  
range. Interestingly, the classifier trained on all the SNPs had a similar performance,  
230  
despite being the only method aiming only at minimizing prediction error. Of course,  
231  
although these performances are low, we do not expect to separate cases from controls  
232  
well using exclusively genetic data [28].  
233

Another desirable quality of a selection algorithm is the stability of the solution with  
234  
respect to small changes in the input (Section 4.5.1). Heinz was highly stable in our  
235  
benchmark, while the other methods displayed similarly low stabilities (Fig 3C).  
236

In terms of computational runtime, the fastest method was heinz (Fig 3D), which  
237  
returned a solution in a few seconds. HotNet2 was the slowest (3 days and 14 hours on  
238  
average). Including the time required to compute the gene scores, however, slows down  
239  
considerably gene-based methods; on this benchmark, that step took on average 1 day  
240  
and 9.33 hours. Including this first step, it therefore took 5 days on average for HotNet2  
241  
to produce a result.  
242

## 2.6 Network topology matters, and might lead to ambiguous 243 results 244

As shown above, and despite their similarities, the network methods produced  
245  
remarkably different solutions. This is due to the fact that each of them models the  
246  
problem differently. Importantly, understanding which assumptions they make allows to  
247  
understand the results more in depth. For instance, the fact that LEAN did not return  
248  
any gene implies that there is no gene such that both itself and its environment are on  
249  
average strongly associated with the disease.  
250

In the GENESIS dataset, heinz’s solution is very conservative, providing a small  
251  
solution with the lowest median P-value (Table 1). By repeatedly selecting this compact  
252  
solution, heinz was the most stable method (Fig 3C). Its conservativeness stems from its  
253  
preprocessing step, which models the gene P-values as a mixture model of a beta  
254  
distribution and a uniform distribution, controlled by an FDR parameter. Due to the  
255  
limited signal at the gene level in this dataset (S2 FigB), only 36 of all the genes retain  
256  
a positive score after that transformation. Yet, this small solution does not provide  
257  
much insight into the susceptibility mechanisms to cancer. Importantly, it ignores genes  
258  
that are associated to cancer in this dataset like *FGFR2*.  
259

On the other end of the spectrum, dmGWAS, HotNet2, and SigMod produced large  
260  
solutions. dmGWAS’ solution is the lowest scoring solution on average. This is due to  
261  
the greedy framework it uses, which has a bias for larger solutions [29]. It considered all  
262  
nodes at distance 2 of the examined subnetwork, and accepted a weakly associated gene  
263  
if it was linked to another, high scoring one. This is exacerbated when the results of  
264  
successive greedy searches are aggregated, leading to a large, tightly connected cluster of  
265  
unassociated genes (Fig 4A). This relatively low signal-to-noise ratio combined with the  
266  
large solution requires additional analyses to draw conclusions, such as enrichment  
267  
analyses. In the same line, HotNet2’s solution is even harder to interpret, being  
268  
composed of 440 genes divided into 135 subnetworks. Lastly, SigMod misses some of the  
269  
highest scoring, breast cancer susceptibility genes in the dataset, like *FGFR2* and  
270  
*TOX3*.  
271

Another peculiarity of network methods is their relationship to degree centrality. We  
272  
studied random rewirings of the PPIN while preserving node centrality (Section 4.5.4).  
273  
In this setting, network methods favored central genes, as they often connect high  
274  
scoring nodes (Fig 4B). This is despite the fact that highly central genes often had no  
275  
association to breast cancer susceptibility (Fig 4C). This was especially the case of  
276

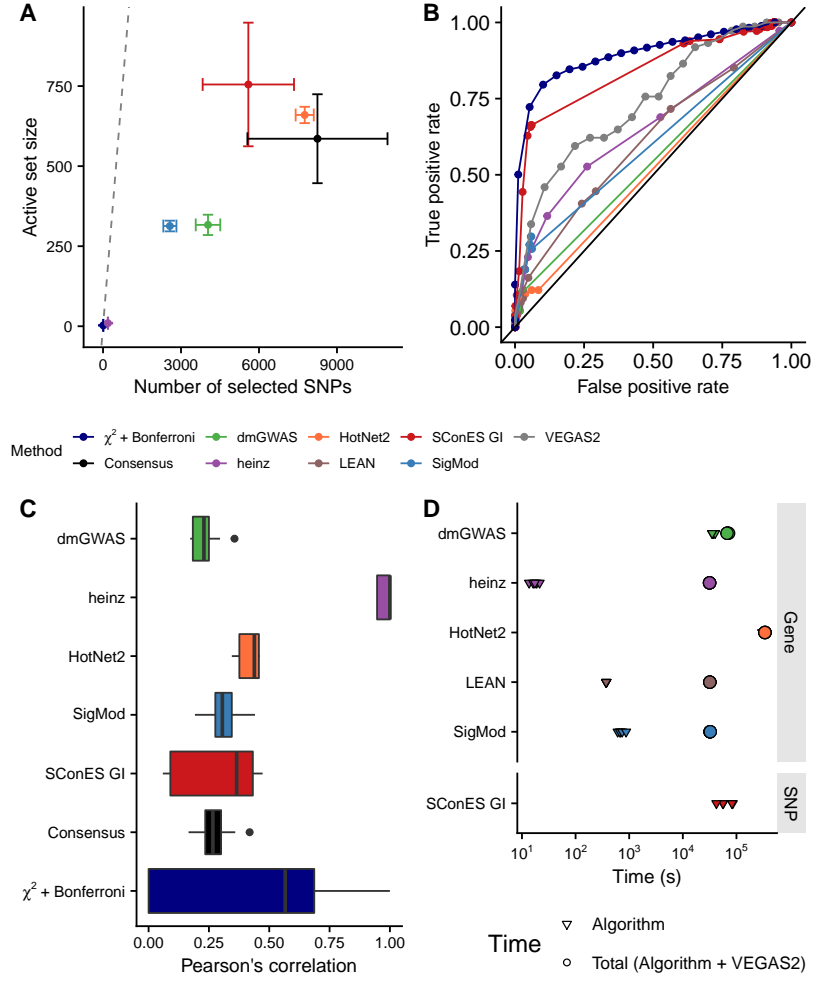


**Fig 3. Comparison of network-based GWAS methods on GENESIS.** Each method was run 5 times on a random subset containing 80% of the samples, and tested on the remaining samples (Section 4.5). As LEAN did not select any gene, it was excluded from all panels except **D**. **(A)** Number of SNPs selected by each method and number of SNPs in the active set found by the classifier (Section 4.5.2). Points are the average over the 5 runs; the error bars represent the standard error of the mean. A grey diagonal line with slope 1 is added for comparison, indicating the upper bound of the active set (i.e. the number of SNPs in the solution). For reference, the active set of Lasso using all the SNPs included, on average, 154 117.4 SNPs. **(B)** True positive rate and true negative rate, using significant SNPs (for SConES and  $\chi^2 + \text{Bonferroni}$ ) and genes (for the remaining methods) in BCAC (Section 4.5.3) as true positives, of multiple parameter combinations for different methods (Section 2.7). **(C)** Pairwise Pearson correlations of the solutions produced by different methods. A Pearson correlation of 1 means the two solutions are the same. A Pearson correlation of 0 means that there is no SNP in common between the two solutions. **(D)** Runtime of the evaluated methods, by type of network used (PPIN or SNP). For gene-based methods, inverted triangles represent the runtime of the algorithm itself, and circles the total time, which includes the algorithm themselves and the additional 119 980 seconds (1 day and 9.33 hours) that VEGAS2 took on average to compute the gene scores from SNP summary statistics.

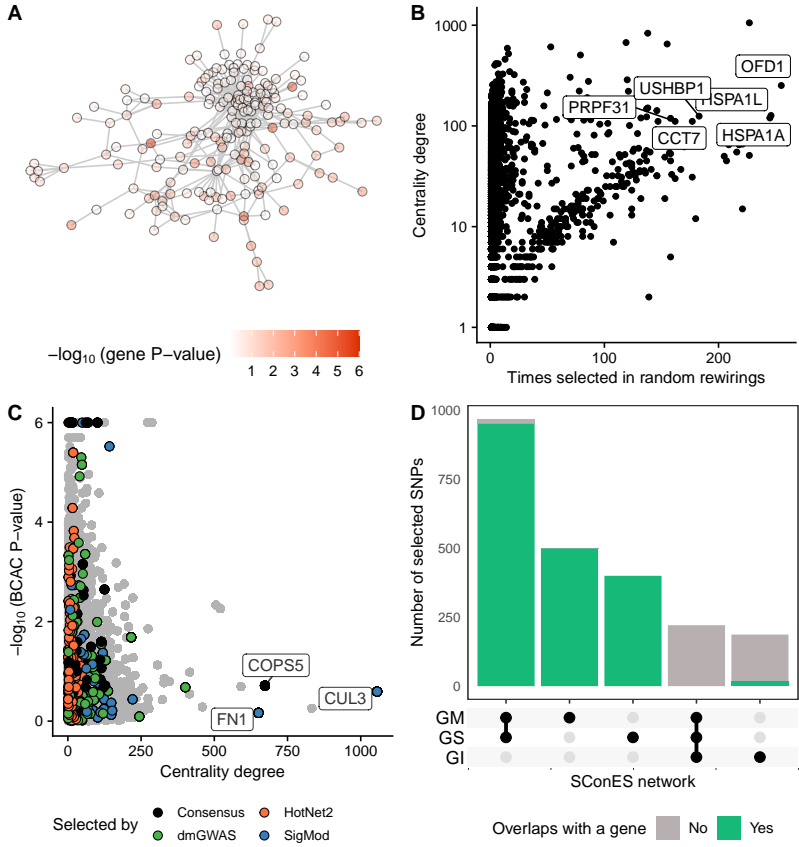


**Fig 4. Drawbacks encountered when using network methods.** (A) DmGWAS solution, with the genes colored according to the  $-\log_{10}$  of their P-value. (B) Centrality degree and  $-\log_{10}$  of the VEGAS2 P-value in BCAC for each of the nodes in the PPIN. We highlighted the genes selected by each method, and the ones selected by more than one (“Consensus”). We labeled the three most central genes that were picked by any method. (C) Number of times a gene was selected by either dmGWAS, heinz, LEAN, or SigMod in 100 rewirings of the PPIN (Section 4.4) and its centrality degree. (D) Overlap between the solutions of SConES GS, GM or GI in the different genomic regions. SNPs that were not selected in the studied network, but were selected in another one, are displayed in background color.

SigMod, which selected three highly central, unassociated genes in both the PPIN and in many of the random rewirings: *COPS5*, *CUL3* and *FN1*. As we showed in Section 2.3, and will show in 2.8, there is evidence in the literature of the contribution of the first two to breast cancer susceptibility. With regards to *FN1*, it encodes a fibronectin, a protein of the extracellular matrix involved in cell adhesion and migration. Overexpression of *FN1* has been observed in breast cancer [30], and it is negatively correlated with poor prognosis in other cancer types [31,32].

By virtue of using a SNP subnetwork, SConES analyzes each SNP in their functional context. It can therefore select SNPs located in genes not included in the PPIN, as well as SNPs in non-coding regions or in non-interacting genes. We compared the solution of SConES in the GI network (using PPIN information), to the one using only positional information (GS network), or positional and gene annotations (GM network). Importantly, SConES produces similar results on the GS and GM networks (S3 Fig). While the solutions on those two greatly overlap with SConES GI's, they contain

additional gene-coding segments (Fig 4C). In fact the formers' solutions are  
chromosome regions related to breast cancer, like 3p24 (*SLC4A7/NEK10* [33]), 5p12  
(*FGF10, MRPS30* [25]), 10q26 (*FGFR2*), and 16q12 (*TOX3*). On top of those SConES  
GS selects region 8q24 (*POU5F1B* [34]).

## 2.7 Different parameters produce similarly-sized solutions

We explored the parameter space of the different methods by running them under  
different combinations of parameters (Section 4.3.4). In agreement with their  
formulations (Section 4.3.3), larger values of certain parameters produce less astringent  
solutions (S6 FigA): for HotNet2 and heinz, we examined the threshold to decide each  
gene has a positive score or zero; for dmGWAS, the  $d$  parameter controls how far  
neighbors could be added; node involved how far the search from the explored  
subnetwork; for SigMod  $nmax$  specifies the maximum size of the solution; and for LEAN,  
it was the P-value threshold to consider a solution significant. Two parameters had the  
opposite effect (larger is more stringent): SigMod's  $maxjump$ , which sets the threshold  
to consider an increment in  $\lambda$  "large enough"; and SConES  $\eta$ , where higher values  
produce more stringent solutions. However, two of the parameters did not have the  
expected effect: dmGWAS'  $r$ , which controls the minimum increment in the score  
required to add an additional gene; and SigMod's  $maxjump$ , which sets the threshold to  
consider an increment in  $\lambda$  "large enough". In both cases, the size of the solution was  
very similar across the different values. Despite the differences in size, the size of the  
solutions was relatively robust to the choice of parameters (S6 FigB).

We computed the Pearson correlation between the different solutions as in Section  
4.5.1 to study how the parameters affected which genes and SNPs were selected (S6  
FigC). This showed that dmGWAS and SigMod are robust to certain parameters:  
dmGWAS' output was mostly determined by the parameter  $d$ , rather than  $r$ ; SigMod's  
by  $nmax$ , rather than  $maxjump$ .

SConES presented an interesting case in terms of feature selection: most of the  
explored combinations of parameters led to trivial solutions (either all the SNPs, or  
none of them were included) (S6 FigA). To explore a more meaningful parameter space,  
we selected the parameters in two rounds. First, we explored the whole sample space.  
Then, we focused in a range of  $\eta$  and  $\lambda$  1.5 orders of magnitude above and below the  
best parameters, respectively. This second parameter space was more diverse, and  
allowed to find more interesting solutions.

## 2.8 Building a stable consensus network preserves global network properties

Most of the network methods, including the consensus, were highly unstable, raising  
questions about the reliability of the results. We built a new, *stable consensus* solution  
using the genes selected most often across the 30 solutions obtained by running the 6  
methods on 5 different splits of the data (Section 4.5). Such a network is expected to  
capture the subnetworks more often found altered, and hence should be more resistant  
to noise. We used only genes selected in at least 7 of the solutions, which corresponded  
to 1% of all genes selected at least once. The resulting stability-based consensus was  
composed of 68 genes (Fig 5). This network shares most of the properties of the  
consensus: breast cancer susceptibility genes are overrepresented ( $P\text{-value} = 3 \times 10^{-4}$ ),  
as well as genes involved in mitochondrial translation and the attenuation phase  
(adjusted  $P$ -values 0.001 and  $3 \times 10^{-5}$  respectively); the selected genes are more central  
than average ( $P\text{-value} = 1.1 \times 10^{-14}$ ); and a considerable number of nodes (19) are  
isolated.

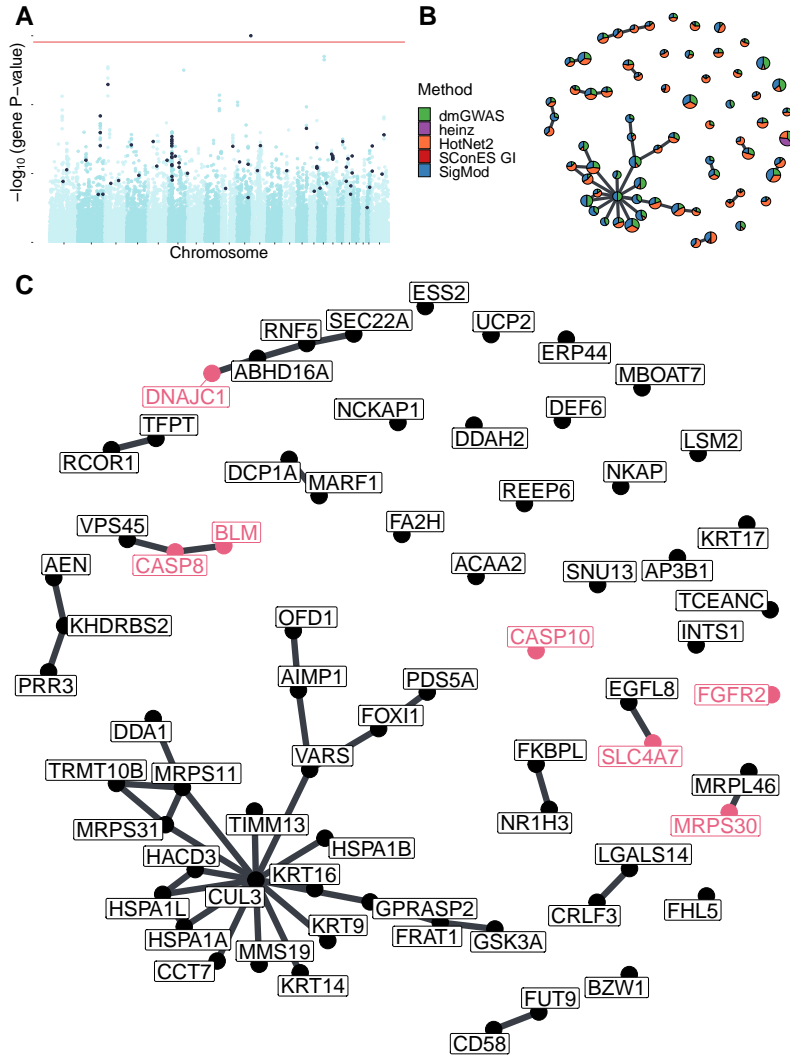


**Fig 5. Stable consensus solution on GENESIS (Section 2.8).** **A** Manhattan plots of genes; in black, the ones in the stable consensus solution. The Bonferroni threshold is indicated by a red line ( $1.53 \times 10^{-6}$  for genes). **B** Stable consensus network. Each gene is represented by a pie chart, which shows the methods that selected it. We enlarged the most central gene (*CUL3*) and those genes that are known breast cancer susceptibility genes and/or significantly associated with breast cancer susceptibility in the BCAC dataset (Section 4.5.3). **C** The nodes are in the same disposition as in panel B, but every gene name is indicated. We colored in pink the names of genes that are known breast cancer susceptibility genes and/or significantly associated with breast cancer susceptibility in the BCAC dataset

Despite these similarities, the consensus and the stable consensus solutions include different genes. In the stable consensus network, the most central gene is *CUL3*, which is absent from the previous consensus solution and has a low association score in both GENESIS and BCAC (P-values of 0.04 and 0.26, respectively). This gene is a component of Cullin-RING ubiquitin ligases. Encouragingly, it impacts the protein levels of multiple genes relevant for cancer progression [35], and its overexpression was also linked to increased sensitivity to carcinogens [36].

### 3 Discussion

In recent years, the ability of GWAS to unravel the mechanisms leading to complex diseases has been called into question [6]. First, the omnigenic model proposes that gene functions are interwoven with each other in a dense co-function network. The practical consequence is that larger and larger GWAS will lead to the discovery of an uninformative wide-spread pleiotropy. Second, discovery in GWAS is hindered by a conservative statistical framework. Network methods elegantly address these two issues by using both association scores and an interaction network to take into consideration the biological context of each of the genes and SNPs. Based on what could be considered diverse interpretations of the omnigenic model, several methods for network-guided discovery have been proposed in recent years. In this article we evaluated the relevance of six of these methods by applying them to the study of GENESIS, a GWAS dataset on familial breast cancer.

DmGWAS, Heinz, HotNet2, SConES and SigMod all yield interesting solutions, which include (but are not limited to) known breast cancer susceptibility genes. In general, the selected genes and SNPs were more central than average, in accordance with the observation that disease genes are more relatively central [9]. However, very central nodes are also more likely to be connecting any given random pair of nodes, making them more likely to be selected by network methods (Section 2.6). Yet, across this article we show that highly central genes that were selected (*COPS5*, *CUL3* and *FN1*) could plausibly be involved in breast cancer susceptibility. Despite these similarities, the solutions obtained were notably different. At one end of the spectrum, SConES and heinz preferred small, highly associated solutions, at the expense of not shedding much light on the etiology of the disease. On the other end, SigMod and dmGWAS gravitate towards larger, less associated solutions which provide a wide overview of the biological context. While this deepens our understanding of the disease and provides biological hypotheses, they require further analyses. For instance, a user might need to examine the centrality of the selected genes, and discern the extent to which that property is driving the selection of each gene. HotNet2 balances both approaches at the expense of producing the largest solution: a constellation of many, highly associated, small subnetworks. Additionally, all solutions share two drawbacks. First, they are all equally bad at discriminating cases from controls. Yet, the classification accuracy of network methods is similar to that of a classifier trained on the entire genome, which suggests that cases and controls are difficult to separate in the GENESIS dataset. This may be due to limited statistical power, which reduces the ability to identify relevant SNPs; but in any event, we do not expect to be able to separate people who have or will developed cancer from others on the sole basis of their genomes, ignoring all environmental factors and chance events. Second, all methods are remarkably unstable, yielding different solutions for slightly different inputs. This might partly be caused by the instability of the P-values themselves in low statistical power settings [37]. Hence, heinz's conservative transformation of P-values, which favors only the most extreme ones, leads to improved stability. Another source of instability might be the redundancy inherent to biological networks, since they are subject to an evolutionary pressure to avoid single points of failure [38]. Hence, biological networks will often have multiple paths connecting two high-scoring nodes.

To overcome these limitations while exploiting the strengths of the individual methods, we proposed combining them into a consensus solution. We use a straightforward strategy of including any node that was recovered by multiple methods. We thus proposed two networks: a consensus solution, meant to address the heterogeneity of the solutions in the full dataset, and a stable consensus solution, which in addition addressed the instability of the methods. They both included the majority of the strongly associated smaller solutions and captured genes and broader mechanisms

related to cancer, thus synthetizing the mechanisms altered in breast cancer cases.  
Thanks to their smaller size and their network structure, they provided compelling  
hypotheses on genes like *COPS5* and *CUL3*, which lack genome-wide association  
with the disease, but are related to cancer at the expression level and interact with genes  
with consistently high association scores. Importantly, while the consensus approach  
was as unstable as the individual network-guided methods, the stable consensus network  
retained the ability to provide compelling hypotheses and had better stability. This  
supports that instability might be caused by redundant but equivalent biological  
mechanisms, and hence validates the conclusions obtained on the individual solutions  
and the consensus.

Across this article, we have compared our results to significant genes and SNPs in  
the BCAC study [19]. Network methods show modest precision, but much higher recall  
at recovering BCAC biomarkers (Section 2.4). While precision might be desirable when  
a subset of good markers is required (for instance, for diagnosis), higher recall is  
desirable in exploratory settings. Nonetheless, BCAC is not an ideal ground truth. First,  
the studied populations are non-overlapping: BCAC focuses on a pan-European cohort,  
while GENESIS targets the French population specifically. Second, the study designs  
differ: a high proportion of breast cancer cases investigated in BCAC are sporadic (not  
selected according to family history), while GENESIS is a homogeneous dataset not  
included in BCAC and which focuses on the French high-risk population attending the  
family cancer clinics. Despite these differences, we expect some degree of shared genetic  
architecture, especially at the gene level. Finally, and this is indeed the motivation for  
this study, GWAS are unlikely to identify all genes relevant for the disease: some might  
only show up in rare-variant studies; others might have too low effect sizes. Network  
methods account for this by including genes with low association scores but with  
relevant topological properties. Hence, network methods and GWAS, even well-powered,  
are unlikely to capture exactly the same sets of genes. This might partly excuse the low  
precisions displayed in Section 2.4 and the low AUC displayed in Section 2.5.

The strength of network-based analyses comes from leveraging prior knowledge to  
boost discovery. In consequence, they show their shortcomings on understudied genes,  
especially those not in the network. Out of the 32 767 genes to which we can map the  
genotyped SNPs, 60.7% (19 887) are not in the PPIN. The majority of those (14 660)  
are non-coding genes, mainly lncRNA, miRNA, and snRNA (S7 Fig). Yet, RNA genes  
like *CASC16* are associated to breast cancer (Section 2.1), reminding us of the  
importance of using networks beyond coding genes. In addition, even protein-coding  
genes linked to breast cancer susceptibility [33], like *NEK10* ( $P$ -value  $1.6 \times 10^{-5}$ ,  
overlapping with *SLC4A7*) or *POU5F1B*, were absent from the PPIN. However, on  
average protein-coding genes absent from the PPIN are less associated with breast  
cancer susceptibility (Wilcoxon rank-sum  $P$ -value =  $2.79 \times 10^{-8}$ , median  $P$ -values of  
0.43 and 0.47). This cannot be due to well-known genes having more known interactions  
because we are only using interactions from high-throughput experiments. As disease  
genes tend to be more central [9], we hypothesize that it is due to interactions between  
central genes being more likely. It is worth noting that network methods that do not  
use PPIs, like SConES GS and GM, did recover SNPs in *NEK10* and *CASC16*.  
Moreover, both SConES GM and GI recovered intergenic regions, which might contain  
key regulatory elements [39] and, yet, are excluded from gene-centric approaches. This  
shows the potential of SNP networks, in which SNPs are linked when there is evidence  
of co-function, to perform network-guided GWAS even in the absence of gene-level  
interactions. Lastly, all the methods are heavily affected by how SNPs are mapped to  
genes, and other strategies (e.g. eQTLs, SNPs associated to the expression of a gene)  
might lead to different results.

As not all databases compile the same interactions, the choice of the PPIN

determines the final output. In this work we used exclusively interactions from HINT  
450  
from high-throughput experiments. This responds to concerns about adding interactions  
451 identified in targeted studies and prone to a “rich getting richer” phenomenon: popular  
452 genes have a higher proportion of their interactions described [40, 41], and they might  
453 bias discovery by reducing the average shortest path length between two random nodes.  
454 On the other hand, Huang et al. [10] found that larger networks were more useful than  
455 smaller networks to identify disease genes. This would support using the largest  
456 networks in our experiments. However, when we compared the impact of using a larger  
457 PPIN containing interactions from both high-throughput experiments and the literature  
458 (Section 4.3.2), we found that for most of the methods it did not greatly change the size  
459 or the stability of the solution, the classification accuracy, or the runtime (S8 Fig). This  
460 supports using only interactions from high-throughput experiments, which produces  
461 apparently similar solutions and avoids falling into “circular reasonings”, where the  
462 best-known genes are artificially pushed into the solutions.  
463

A crucial step for the gene-based methods is the computation of the gene score. In  
464 this work we used VEGAS2 [42] due to the flexibility it offers to use user-specified gene  
465 annotations. However, it presents known problems (selection of an appropriate  
466 percentage of top SNPs, long runtimes and P-value precision limited to the number of  
467 permutations [43]), and other algorithms like PEGASUS [43], SKAT [44] or  
468 COMBAT [45] might have more statistical power.  
469

How to handle linkage disequilibrium (LD) is often a concern among GWAS  
470 practitioners. VEGAS2 accounts for LD patterns, and hence an LD pruning step would  
471 not impact gene-based network methods, although it would speed up VEGAS2’s  
472 computation time. With regards to SConES, fewer SNPs would lead to simpler SNP  
473 networks and, possibly, shorter runtimes. However, as mentioned in Section 2.6, LD  
474 patterns seem to drive SConES’ solutions, and an LD pruning step could potentially  
475 alter them. In Section 2.3 we highlight ambiguities that appear when genes overlap or  
476 are in LD. In fact, the presented case is paradigmatic, since all three genes are located  
477 in the HLA region, the most gene-dense region of the genome [46]. Network methods  
478 are prone to selecting such genes when they are functionally related, and hence  
479 interconnected in the PPIN. But the opposite case is also true: when genes are not  
480 functionally related (and hence disconnected in the PPIN), network methods might  
481 disregard them even if they have high association scores. LD also affects SConES, since  
482 it penalizes selecting a SNP and not its neighbors, via a nonzero parameter  $\eta$  in  
483 Equation 5. Due to LD, nearby SNPs’ P-values are correlated; and since SNP networks  
484 are determined by positional information, nearby SNPs are likely to be linked. Hence,  
485 SConES will tend to select LD-blocks formed by low P-value SNPs. This might explain  
486 why SConES produces similar results on the GS and GM networks, heavily affected by  
487 LD (Section 2.6). However, this same behavior raises the burden of proof required to  
488 select SNPs with many interactions, like those mapped to hub genes in the PPIN. For  
489 this reason, SConES GI did not select any protein coding gene. We hypothesize that  
490 this is caused by the absence of joint association of a gene and a majority of its  
491 neighbors. This is supported by the lack of results from LEAN as well. Yet, a different  
492 combination of parameters could lead to a more informative SConES’ solution (e.g. a  
493 lower  $\lambda$  in Equation 5), although it is unclear how to find it. In addition, due to the  
494 design of the iCOGS array (Section 4.1), the genome of GENESIS participants has not  
495 been unbiasedly surveyed: some regions are fine-mapped — which might distort gene  
496 structure in GM and GI networks — while others are under studied — hindering the  
497 accuracy with which the GS network captures the genome structure. A stringent LD  
498 pruning might address such problems.  
499

To produce the two consensus solutions, we had to face practical challenges due to  
500 the differences in interfaces, preprocessing steps, and unexpected behaviors of the  
501

various methods. To make it easier for other to apply these methods to new datasets and aggregate their solutions, we built six nextflow pipelines [47] with a consistent interface and, whenever possible, parallelized computation. They are available on GitHub: <https://github.com/hclimente/gwas-tools> (Section 4.1). Importantly, those methods that had a permissive license were compiled into a Docker image for easier use, which is available on Docker Hub hclimente/gwas-tools.

## 4 Materials and methods

### 4.1 GENESIS dataset, preprocessing and quality control

The GENE Sisters (GENESIS) study was designed to investigate risk factors for familial breast cancer in the French population [18]. Index cases are patients with infiltrating mammary or ductal adenocarcinoma, who had a sister with breast cancer, and who have been tested negative for *BRCA1* and *BRCA2* pathogenic variants. Controls are unaffected colleagues and/or friends of the cases, born around the year of birth of their corresponding case ( $\pm 3$  years). We focused on the 2 577 samples of European ancestry, of which 1 279 were controls and 1 298 were cases. The genotyping was performed using the iCOGS array, a custom Illumina array designed to study the genetic susceptibility to hormone-related cancers [48]. It contains 211 155 SNPs, including SNPs putatively associated with breast, ovarian, and prostate cancers, SNPs associated with survival after diagnosis, and SNPs associated to other cancer-related traits, as well as candidate functional variants in selected genes and pathways.

We discarded SNPs with a minor allele frequency lower than 0.1%, those not in Hardy–Weinberg equilibrium in controls ( $P$ -value  $< 0.001$ ), and those with genotyping data missing on more than 10% of the samples. A subset of 20 duplicated SNPs in *FGFR2* were also removed. In addition, we removed the samples with more than 10% missing genotypes. After controlling for relatedness, 17 additional samples were removed (6 for sample identity error, 6 controls related to other samples, 2 cases being related to an index case, and 3 additional controls having a high relatedness score). Lastly, based on study selection criteria, 11 other samples were removed (1 control having cancer, 4 index cases with no affected sister, 3 half-sisters, 1 sister with lobular carcinoma *in situ*, 1 with a *BRCA1* or *BRCA2* pathogenic variant detected in the family, 1 with unknown molecular diagnosis). The final dataset included 1 271 controls and 1 280 cases, genotyped over 197 083 SNPs.

We looked for population structure that could produce spurious associations. A principal component analysis revealed no visual differential population structure between cases and controls (S1 Fig). Independently, we did not find evidence of genomic inflation ( $\lambda = 1.05$ ) either, further confirming the absence of confounding population structure.

### 4.2 SNP- and gene-based GWAS

To measure association between a genotype and susceptibility to breast cancer, we performed a per-SNP 1 d.f.  $\chi^2$  allelic test using PLINK v1.90 [49]. In order to obtain significant SNPs, we performed Bonferroni correction, to keep family-wise error rate below 5%. The threshold used was  $\frac{0.05}{197083} = 2.54 \times 10^{-7}$ .

Then, we used VEGAS2 [42] to compute the gene-level association score from the  $P$ -values of the SNPs mapped to them. More specifically, we mapped SNPs to genes through their genomic coordinates: all SNPs located within the boundaries of a gene,  $\pm 50$  kb, were mapped to that gene. For each gene, we computed VEGAS2 scores using only the 10% of SNPs with lowest  $P$ -values among all those that were mapped to it. We

used the 62 193 genes described in GENCODE 31 [50], although only 54 612 could be mapped to at least one SNP. Out of those, we focused exclusively on the 32 767 that had a gene symbol. Out of the 197 083 SNPs remaining after quality control, 164 037 were mapped to at least one of these genes. We also used Bonferroni correction to obtain significant genes; in this case, the threshold of significance was  $\frac{0.05}{32767} = 1.53 \times 10^{-6}$ .

## 4.3 Network methods

### 4.3.1 Mathematical notations

In this article, we use undirected, vertex-weighted networks, or graphs,  $G = (V, E, w)$ .  $V = \{v_1, \dots, v_n\}$  refers to the vertices, with weights  $w : V \rightarrow \mathbb{R}$ . Equivalently,  $E \subseteq \{\{x, y\} | x, y \in V \wedge x \neq y\}$  refers to the edges. When referring to a subnetwork  $S$ ,  $V_S$  is the set of nodes in  $S$  and  $E_S$  is the set of edges in  $S$ . A special case of subgraphs are *connected* subgraphs, which occur when every node in the subgraph can be reached from any other node.

Nodes can be described by properties provided by the topology of the graph. We focus on two of those: degree centrality, and betweenness centrality. The degree centrality, or degree, is the number of edges that a node has. The betweenness centrality, or betweenness, is the number of times a node participates in the shortest paths between two other nodes.

We also use two matrices that describe two different properties of a graph. These matrices are square, and have as many rows and columns as nodes in the network. The element  $(i, j)$  hence represents a relationship between  $v_i$  and  $v_j$ . The *adjacency matrix*  $W_G$  contains a 1 when the corresponding nodes are connected, and 0 otherwise; its diagonal is zero. The *degree matrix*  $D_G$  is a diagonal matrix which contains the degree of the different nodes.

### 4.3.2 Networks

**Gene network** The mathematical formulations of the different network methods are compatible with any type of network (protein interactions, gene coexpression, regulatory, etc.). Here, we used protein-protein interaction networks (PPIN) for all of them except SConES, as PPINs are interpretable, well-characterized, and the methods were designed to run efficiently on them. We built our PPIN from both binary and co-complex interactions stored in the HINT database (release April 2019) [41]. Unless otherwise specified, we used only interactions coming from high-throughput experiments, leaving out targeted studies that might bias the topology of the PPIN. Out of the 146 722 interactions from high-throughput experiments that HINT stores, we were able to map 142 541 to a pair of gene symbols, involving 13 619 genes. 12 880 of those mapped to a genotyped SNP after quality control, involving 127 604 interactions. The scoring function for the nodes changed from method to method (Section 4.3.3).

Additionally, we compared the results obtained on the aforementioned PPIN with those obtained on another PPIN built using interactions coming from both high-throughput and targeted studies. In that case, out of the 179 332 interactions in HINT, 173 797 mapped to a pair of gene symbols. Out of those, 13 735 mapped to a genotyped SNP after quality control, involving 156 190 interactions.

**SNP networks** SConES [16] is the only network method designed to handle SNP networks. As in gene networks, two SNPs are connected in a SNP network when there is evidence of shared functionality between two SNPs. Azencott et al. [16] proposed three ways of building these networks: connecting the SNPs consecutive in the genomic sequence (“GS network”); interconnecting all the SNPs mapped to the same gene, on

top of GS (“GM network”); and interconnecting all SNPs mapped to two genes for which a protein-protein interaction exists, on top of GM (“GI network”). We focused on the GI network, as it fits the scope of this work better, using the PPIN described above. However, at different stages we also compared GI to GS and GM to understand how considering the PPIN affects SConES’ output. For the GM network, we used the mapping described in Section 4.3.5. In all three the node scores are the association scores of the individual SNPs with the phenotype (1 d.f.  $\chi^2$  statistic). The properties of these three subnetworks are available in S1 Table.

#### 4.3.3 High-score subnetwork search algorithms

Genes that contribute to the same function are nearby in the PPIN, and can be topologically related to each other in diverse ways (densely interconnected modules, nodes around a hub, a path, etc.). Several aspects have to be taken into consideration when developing a network method: how to score the nodes, whether the affected mechanisms form a single connected component or several, how to frame the problem in a computationally efficient fashion, which network to use, etc. Unsurprisingly, multiple solutions have been proposed. We examined six of them: five that explore the PPIN, and one which explores SNP networks. We selected methods that were open-source, and had an implementation available and accessible documentation. Their main differences are summarized in Table 2. We scored both SNPs and genes with the P-values (or transformations of them) computed in Section 4.2.

**Table 2. Summary of the differences between the network methods.**

Method	Field	Nodes	Exhaustive	Solution	Comp.	Input	Scoring	Ref.
dmGWAS	GWAS	Genes	No	-	1	Summary	$-\log_{10}(P)$	[13]
heinz	Omics	Genes	Yes	-	1	Summary	BUM	[14]
HotNet2	Omics	Genes	Yes	Module	$\geq 1$	Summary	Local FDR	[15]
LEAN	Omics	Genes	Yes	Star	$\geq 1$	Summary	$-\log_{10}(P)$	[12]
SConES	GWAS	SNPs	Yes	Module	$\geq 1$	Genotypes	1 d.f. $\chi^2$	[16]
SigMod	GWAS	Genes	Yes	Module	$\geq 1$	Summary	$\Phi^{-1}(1 - P)$	[17]

**Field:** field in which the algorithm was developed. **Nodes:** the type of nodes in the network, either genes (PPIN) or SNPs. **Exhaustive:** whether all the possible solutions given the selected hyperparameters are explored. **Solution:** additional properties are enforced on the solution, other than containing high scoring, connected nodes. **Comp.:** number of connected components in the solution. **Input:** genotype data or GWAS summary statistics. **Scoring:** how SNP/gene P-values are transformed into node scores. In the case of heinz, BUM stands for beta-uniform model, used to transform the P-values; for SigMod,  $\Phi^{-1}$  represents the inverse of the cumulative distribution function of the standard Normal distribution. **Ref.:** original publication featuring the algorithm.

**dmGWAS** dmGWAS seeks the subgraph with the highest local density in low P-values [13]. To that end it searches candidate solutions using a greedy, “seed and extend”, heuristic:

1. Select a seed node  $i$  and form the subnetwork  $S_i = \{i\}$ .
2. Compute Stouffer’s Z-score  $Z_m$  for  $S_i$  as

$$Z_m = \frac{1}{\sqrt{k}} \sum_{j \in S_i} z_j, \quad (1)$$

where  $k$  is the number of genes in  $S_i$ ;  $z_j$  is the Z score of gene  $j$ , computed as  $\phi^{-1}(1 - P\text{-value}_j)$ ; and  $\phi^{-1}$  is the inverse normal distribution function.

- 623
3. Identify neighboring nodes of  $S_i$ , i.e. nodes at distance  $\leq d$ .

624

  4. Add the neighboring nodes whose inclusion increases  $Z_{m+1}$  by more than a threshold  $Z_m \times (1 + r)$ .

625

  5. Repeat 2-4 until no further enlargement is possible.

626

  6. Add  $S_i$  to the list of subnetworks to return. Normalize its Z-score as

627

$$Z_N = \frac{Z_m - \text{mean}(Z_m(\pi))}{\text{SD}(Z_m(\pi))}, \quad (2)$$

where  $Z_m(\pi)$  represents a vector containing 100 000 random subsets of the same number of genes.

628  
629

DmGWAS carries out this process on every gene in the PPIN. We used the implementation of dmGWAS in the dmGWAS 3.0 R package [51]. Unless otherwise specified, we used the suggested hyperparameters  $d = 2$  and  $r = 0.1$ . We used the function `simpleChoose` to select the solution, which aggregates the top 1% subnetworks.

630  
631  
632  
633  
634

**heinz** The goal of heinz is to identify the highest-scored connected subnetwork [14]. The authors propose a transformation of the genes' P-value into a score that is negative under weak association with the phenotype, and positive under a strong one. This transformation is achieved by modeling the distribution of P-values by a beta-uniform model (BUM) parameterized by the desired false discovery rate (FDR). Thus formulated, the problem is NP-complete, and hence solving it would require a prohibitively long computational time. To solve it efficiently it is re-cast as the Prize-Collecting Steiner Tree Problem (PCST), which seeks to select the connected subnetwork  $S$  that maximizes the *profit*  $p(S)$ , defined as:

635  
636  
637  
638  
639  
640  
641  
642  
643

$$p(S) = \sum_{v \in V_S} p(v) - \sum_{e \in E_S} c(e). \quad (3)$$

were  $p(v) = w(v) - w'$  is the *profit* of adding a node,  $c(e) = w'$  is the *cost* of adding an edge, and  $w' = \min_{v \in V_G} w(v)$  is the smallest node weight of  $G$ . All three are positive quantities. Heinz implements the algorithm from Ljubić et al. [52] which, in practice is often fast and optimal, although neither is guaranteed. We used BioNet's implementation of heinz [53, 54].

644  
645  
646  
647  
648

**HotNet2** HotNet2 was developed to find connected subgraphs of genes frequently mutated in cancer [15]. To that end, it considers both the local topology of the PPIN and the scores of the nodes. The former is captured by an insulated heat diffusion process: at initialization, the score of the node determines its initial heat; iteratively each node yields heat to its "colder" neighbors, and receives heat from its "hotter" neighbors while retaining part of its own (hence, *insulated*). This process continues until a stationary state is reached, in which the temperature of nodes does not change anymore, and results in a diffusion matrix  $F$ .  $F$  is used to compute the similarity matrix  $E$  that models exchanged heat as

649  
650  
651  
652  
653  
654  
655  
656  
657

$$E = F \text{diag}(w(V)), \quad (4)$$

where  $\text{diag}(w(V))$  is a diagonal matrix with the node scores in its diagonal. For any two nodes  $i$  and  $j$ ,  $E_{ij}$  models the amount of heat that diffuses from node  $j$

658  
659

to node  $i$ , which can be interpreted as a (non-symmetric) similarity between those two nodes. To obtain densely connected solutions, HotNet2 prunes  $E$ , only preserving edges such that  $w(E) > \delta$ . Lastly, HotNet2 evaluates the statistical significance of the solutions by comparing their size to the size of PPINs obtained by permuting the node scores. We assigned initial node scores as in Nakka et al. [43], assigning a score of 0 for the genes with a low probability of being associated to the disease, and  $-\log_{10}(\text{P-value})$  to those likely to be. In the GENESIS dataset, the threshold separating both was a P-value of 0.125, which was obtained using a local FDR approach [55]. HotNet2 has two parameters: the restart probability  $\beta$ , and the threshold heat  $\delta$ . Both parameters are set automatically by the algorithm, which is robust to their values [15]. HotNet2 is implemented in Python [56].

**LEAN** LEAN searches altered “star” subnetworks, that is, subnetworks composed by one central node and all its interactors [12]. By imposing this restriction, LEAN can exhaustively test all such subnetworks (one per node). For a particular subnetwork of size  $m$ , the P-values corresponding to the involved nodes are ranked as  $p_1 \leq \dots \leq p_m$ . Then,  $k$  binomial tests are conducted, to compute the probability of having  $k$  out of  $m$  P-values lower or equal to  $p_k$  under the null hypothesis. The minimum of these  $k$  P-values is the score of the subnetwork. This score is transformed into a P-value through an empirical distribution obtained via a subsampling scheme, where gene sets of the same size are selected randomly, and their score computed. Lastly, P-values are corrected for multiple testing through a Benjamini-Hochberg correction. We used the implementation of LEAN from the LEANR R package [57].

**SConES** SConES searches the minimal, modular, and maximally associated subnetwork in a SNP graph [16]. Specifically, it solves the problem

$$\arg \max_{S \subseteq G} \underbrace{\sum_{v \in V_S} w(v)}_{\text{association}} - \lambda \underbrace{\sum_{v \in V_S} \sum_{u \notin V_S} W_{vu}}_{\text{connectivity}} - \underbrace{\eta |V_S|}_{\text{sparsity}} \quad (5)$$

where  $\lambda$  and  $\eta$  are hyperparameters that control the sparsity and the connectivity of the model. The connectivity term penalizes disconnected solutions, with many edges between nodes that are selected and nodes that are not. Given a  $\lambda$  and an  $\eta$ , the aforementioned problem has a unique solution, that SConES finds using a graph min-cut procedure. As in Azencott et al. [16], we selected  $\lambda$  and  $\eta$  by cross-validation, choosing the values that produce the most stable solution across folds. In this case, the selected hyperparameters were  $\eta = 3.51$ ,  $\lambda = 210.29$  for SConES GS;  $\eta = 3.51$ ,  $\lambda = 97.61$  for SConES GM; and  $\eta = 3.51$ ,  $\lambda = 45.31$  for SConES GI. We used the version on SConES implemented in the R package `martini` [58].

**SigMod** SigMod aims at identifying the highest-scoring, most densely connected subnetwork [17]. It addresses an optimization problem similar to that of SConES (Equation 5), but the connectivity term encourages connected solutions by favoring solutions where many edges connect two selected nodes, rather than penalizing disconnected ones.

$$\arg \max_{S \subseteq G} \underbrace{\sum_{v \in V_S} w(v)}_{\text{association}} + \lambda \underbrace{\sum_{v \in V_S} \sum_{u \in V_S} W_{vu}}_{\text{connectivity}} - \underbrace{\eta |V_S|}_{\text{sparsity}} . \quad (6)$$

As for SConES, this optimization problem can also be solved by a graph min-cut approach.

SigMod presents three important differences with SConES. First, it is designed for PPINs. Second, it favors solutions containing many edges. SConES, instead, penalizes connections between the selected and unselected nodes. Third, it explores the grid of hyperparameters differently, and processes their respective solutions. Specifically, for the range of  $\lambda = \lambda_{\min}, \dots, \lambda_{\max}$  for the same  $\eta$ , it prioritizes the solution with the largest change in size from  $\lambda_n$  to  $\lambda_{n+1}$ . Additionally, that change needs to be larger than a user specified threshold `maxjump`. Such a large change implies that the network is densely interconnected. This results in one candidate solution for each  $\eta$ , which are processed by removing any node not connected to any other. A score is assigned to each candidate solution by summing their node scores and normalizing by size. The candidate solution with the highest standardized score and that is not larger than a user-specified threshold (`nmax`) is the chosen solution. SigMod is implemented in an R package [59].

**Consensus** We built a consensus solution by retaining the genes that were selected by at least two of the six methods (using SConES GI for SConES). Any edge between the selected genes in the PPIN was included.

We performed all the computations in the cluster described in Section 4.6.

#### 4.3.4 Parameter space

We used the network methods with the parameters recommended by their authors, or with the default parameters in their absence. Additionally, we explored the parameter space of the different methods to study how they alter the output.

**dmGWAS** We tested multiple values for  $r$  (0.0001, 0.001, 0.01, 0.05, 0.1, 0.25, 0.5, and 1) and  $d$  (1, 2, and 3).

**heinz** We tested multiple FDR thresholds (0.05, 0.1, 0.15, 0.2, 0.25, 0.3, 0.35, 0.4, 0.45, 0.5, 0.55, 0.6, 0.65, 0.7, 0.75, 0.8, 0.85, 0.9, 0.95, 1).

**HotNet2** We tested different thresholds to decide which genes would receive a score of 0, and which ones a score of  $-\log_{10}(\text{P-value})$ : 0.001, 0.01, 0.05, 0.125, 0.25, and 0.5.

**LEAN** We used the following significance cutoffs for LEAN's P-values (0.05, 0.1, 0.15, 0.2, 0.25, 0.3, 0.35, 0.4, 0.45, 0.5, 0.55, 0.6, 0.65, 0.7, 0.75, 0.8, 0.85, 0.9, 0.95, and 1).

**SConES** We used the values of  $\lambda$  and  $\eta$  that `martini` explores (35.54, 5.40, 0.82, 0.12, 0.02, 0.01, 4.39e-4, 6.68e-5, 1.02e-5, and 1.55e-6 in both cases)

**SigMod** We tested multiple values for the parameters `nmax` (10, 50, 100, 300, 700, 1000, and 10 000) and `maxjump` (5, 10, 20, 30, and 50).

#### 4.3.5 Comparing SNP-methods to gene-methods, and vice versa

In multiple steps of this article, we needed to compare the outcome of a method that works on genes with the outcome of another method that works on SNPs. For this purpose, we used the SNP-gene correspondence described in Section 4.2. To convert a list of SNPs into a list of genes, we included all the genes that can be mapped to any of the SNPs. Conversely, to convert a list of genes into a list of SNPs, we included all the SNPs that can be mapped to any of the genes.

## 4.4 Pathway enrichment analysis

We searched for pathways enriched in the gene solutions produced by the above methods. We conducted a hypergeometric test on pathways from Reactome [60] using the function `enrichPathway` from the ReactomePA R package [61]. The universe of genes included any gene that we could map to a SNP in the iCOGS array (Section 4.2). We adjusted the P-values for multiple testing as in Benjamini and Hochberg [62] (BH). Pathways with a BH adjusted P-value < 0.05 were deemed significant.

## 4.5 Benchmark of methods

We evaluated multiple properties (described below) of the different methods through a 5-fold subsampling setting. We applied each method to 5 random subsets of the original GENESIS dataset containing 80% of the samples (*train set*). When pertinent, we evaluated the solution on the remaining 20% (*test set*). We used the 5 repetitions to estimate the average and the standard deviation of the different measures. Every method and repetition ran on the same computational settings (Section 4.6).

### 4.5.1 Properties of the solution

We compared the runtime, the number of selected features (genes or SNPs), and the stability (sensitivity of the result to small changes in the input, here, using different *train* sets) of the different network methods. Nogueira and Brown [63] proposed quantifying the stability of a method using the Pearson correlation between the genes selected on different subsamples. This correlation was calculated between vectors with the length of the total number of features, containing a 0 at position  $i$  if feature  $i$  was not selected, and 1 if it was.

### 4.5.2 Classification accuracy of selected SNPs

A desirable solution offers good predictive power on unseen *test* samples. We evaluated the predicting power of the SNPs selected by the different methods through the performance of an L1-penalized logistic regression classifier, which searches for a small subset of SNPs which provides good classification accuracy. We trained the classifier exclusively on those selected SNPs to predict the outcome (case/control). The L1 penalty helps to account for linkage disequilibrium by reducing the number of SNPs included in the model (*active set*) while improving the generalization of the classifier. This penalty was set by cross-validation, choosing the value that minimized misclassification error. We applied each network method to each *train* set, and trained the classifier on the same train set using only the selected SNPs. When the method retrieved a list of genes (all of them except SConES), we considered as selected all the SNPs mapped to any of those genes. Then we evaluated the sensitivity and the specificity on the *test set*. The active set gave an estimate of a plausible, more sparse solution with comparable predictive power to the original solution. To obtain a baseline, we also trained the classifier on all the SNPs. We do not expect a linear model on selected SNPs to be able to separate cases from controls well. Indeed, the lifetime cumulative incidence of breast cancer among women with a family history of breast or ovarian cancer, and no *BRCA1/2* mutations, is only 3.9 times more than in the general population [64]. However, classification accuracy may be one additional informative criterion on which to evaluate solutions.

#### 4.5.3 Comparison to state-of-the-art

An alternative way to evaluate the results is by comparing our results to an external dataset. For that purpose, we used the 153 genes associated to familial breast cancer on DisGeNET [65]. Across this article we refer to these genes as *breast cancer susceptibility genes*.

Additionally, we used the summary statistics from the Breast Cancer Association Consortium (BCAC), a meta-analysis of case-control studies conducted in multiple countries which included 13 250 641 SNPs genotyped or imputed on 228 951 women of European ancestry mostly from the general population [19]. Through imputation, BCAC includes more SNPs than the iCOGS array used for GENESIS (Section 4.1). Yet, in all the comparisons in this paper, we focused on the subset of the GENESIS SNPs that passed quality control (Section 4.1). Hence, we used the same Bonferroni threshold as in Section 4.2 to determine the significant SNPs in BCAC. We also computed gene-scores in the BCAC data using VEGAS2, as in Section 4.1. In this case, we did use the summary statistics of all 13 250 641 available SNPs, and the genotypes from European samples from the 1000 Genomes Project [66] to compute the LD patterns. Since these genotypes did not include chromosome X, we excluded it from this analysis. All comparisons included only the genes common to GENESIS and BCAC, so we used the corresponding Bonferroni threshold ( $1.66 \times 10^{-6}$ ) to call gene significance.

#### 4.5.4 Network rewirings

Rewiring the PPIN while preserving the number of edges of each gene allows to study the impact of the topology on the output of network methods. Indeed, the edges lose their biological meaning but the topology of the network is conserved. We produced 100 such rewirings by swapping edges in the PPIN. We scored the genes as described in section 4.3.3. We only applied only four methods on the rewirings: heinz, dmGWAS, LEAN and SigMod. We excluded HotNet2 and SConES, since they take notably longer to run than the other methods, while taking up more computational resources.

### 4.6 Computational resources

We ran all the computations on a Slurm cluster, running Ubuntu 16.04.2 on the nodes. The CPU models on the nodes were Intel Xeon CPU E5-2450 v2 at 2.50GHz and Intel Xeon E5-2440 at 2.40GHz. The nodes running heinz and HotNet2 had 20GB of memory; the ones running dmGWAS, LEAN, SConES, and SigMod, 60GB. For the benchmark (Section 4.5), we ran each of the methods on the same Ubuntu 16.04.2 node, with a CPU Intel Xeon E5-2450 v2 at 2.50GHz, and 60GB of memory.

### 4.7 Code and data availability

We developed computational pipelines for several steps of GWAS analyses, such as physically mapping SNPs to genes, computing gene scores, and performing six different network analyses. For each of those processes, we created a pipeline with a clear interface that should work on any GWAS dataset. They are compiled in <https://github.com/hclimente/gwas-tools>. Although the GENESIS data is not public, the code to apply the pipelines to this data, as well as the code that reproduces all the analyses in this article are available at <https://github.com/hclimente/genewa>. We deposited all the produced gene solutions on NDEX (<http://www.ndexbio.org>), under the UUID e9b0e22a-e9b0-11e9-bb65-0ac135e8bacf.

Summary statistics for SNPs and genes are available at <https://github.com/hclimente/genewa>. We cannot share genotype data publicly

for confidentiality reasons, but are available from GENESIS. Interested researchers can contact nadine.andrieu(at)curie.fr.

## 5 Supporting information

**S1 Table. Summary statistics on the results of SConES on the three SNP-SNP interaction networks.** The first row within each block contains the summary statistics on the whole network.

**S2 Table. Summary statistics on the results of multiple network methods on the PPIN.** The first row contains the summary statistics on the whole PPIN.

**S3 Table. Pathway enrichment analyses of the genes in SigMod solution.**

**S4 Table. Pathway enrichment analyses of the genes in dmGWAS solution.**

**S5 Table. Pathway enrichment analyses of the genes in HotNet2 solution.**

**S6 Table. Pathway enrichment analyses of the genes in the consensus solution.**

**S1 Fig. GENESIS shows no differential population structure between cases and controls. (A,B,C,D)** Eight main principal components computed on the genotypes of GENESIS. Cases are colored in green, controls in orange.

**S2 Fig. Association in GENESIS. The red line represents the Bonferroni threshold. (A)** SNP association, measured from the outcome of a 1 d.f.  $\chi^2$  allelic test (Section 4.2). Significant SNPs that are within a coding gene, or within 50 kilobases of its boundaries, are annotated. The Bonferroni threshold is  $2.54 \times 10^{-7}$ . **(B)** Gene association, measured by P-value of VEGAS2 [42] using the 10% of SNPs with the lowest P-values (Section 4.2). The Bonferroni threshold is  $1.53 \times 10^{-6}$ . **(C)** SNP association as in panel (A). The SNPs in black are selected by a L1-penalized logistic regression (Section 4.5.2,  $\lambda = 0.03$ ).

**S3 Fig. Pearson correlation between the different solutions.**

**(A)** Correlation between selected SNPs. **(B)** Correlation between selected genes. In general, the solutions display a very low overlap.

**S4 Fig. Relationship between the  $\log_{10}$  of the betweenness centrality and the  $-\log_{10}$  of the VEGAS2 P-value of the genes in the consensus solution.** The blue line represents a fitted generalized linear model.

**S5 Fig. Additional benchmarks of the network methods** **(A)** Precision and recall of the evaluated methods with respect to Bonferroni-significant SNPs/genes in BCAC. For reference, we added a gray line with a slope of 1. This panel is identical to Fig 2. **(B)** Sensitivity and specificity on the test set of the L1-penalized logistic regression trained on the features selected by each of the methods. The performance of the classifier trained on all SNPs is also displayed. Points are the average over the 5 runs; the error bars represent the standard error of the mean.

**S6 Fig. Parameter space of the network methods.** (A) Boxplot of the solution sizes of the methods under the explored parameters (Section 4.3.4). (B) Size of SConES's with regards to each pair of parameters. (C) Pearson correlation between the solutions of the different runs.

874  
875  
876  
877

**S7 Fig. Biotypes of genes from the annotation that are not present in the HINT PPIN.**

878  
879

**S8 Fig. Comparison of the benchmark on high-throughput (HT) interactions to the benchmark on both high-throughput and literature curated interactions (HT+LC).** Grey lines represent no change in the statistic between the benchmarks (1 for ratios mean(HT) / mean(HT + LC), 0 for differences mean(HT) - mean(HT + LC)). (A) Ratios of the selected features between both benchmarks and of the active set (Section 4.5.2). (B) Shifts in sensitivity and specificity. (C) Shift in Pearson correlation between benchmarks. (D) Ratio between the runtimes of the benchmarks. For gene-based methods, inverted triangles represent the ratio of runtimes of the algorithms themselves, and circles the total time, which includes the algorithm themselves and the additional 119 980 seconds (1 day and 9.33 hours) that VEGAS2 took on average to compute the gene scores from SNP summary statistics. In general, adding additional interactions slightly improves the stability of the solution, but increases the solution size, has mixed effects on the sensitivity and specificity, and impacts negatively the required runtime of the algorithms.

880  
881  
882  
883  
884  
885  
886  
887  
888  
889  
890  
891  
892  
893

**S9 Fig. Overview of the solutions produced by the SConES on the GS and GM networks (Section 4.3.2) on the GENESIS dataset.** (A) Manhattan plots of SNPs (Section 4.2); in black, the method's solution. The Bonferroni threshold ( $2.54 \times 10^{-7}$ ) is indicated by a red line. (B) Precision and recall of the evaluated methods with respect to Bonferroni-significant SNPs (SConES) or genes (other methods) in BCAC. For reference, we added a gray line with a slope of 1. (C) Solution networks.

894  
895  
896  
897  
898  
899  
900

## Acknowledgments

We wish to thank Om Kulkarni for helpful discussion on gene-based GWAS and PPIN databases, and the genetic epidemiology platform (the PIGE, Plateforme d'Investigation en Génétique et Epidemiologie: S. Eon-Marchais, M. Marcou, D. Le Gal, L. Toulemonde, J. Beauvallet, N. Mebirouk, E. Cavaciuti), the biological resource centre (S. Mazoyer, F. Damiola, L. Barjhoux, C. Verny-Pierre, V. Sornin). We wish to pay a tribute to Olga M. Sinilnikova, who was one of the initiators and principal investigators of GENESIS and who died prematurely on June 30, 2014.

901  
902  
903  
904  
905  
906  
907

We thank all the GENESIS collaborating cancer clinics clinics (Clinique Sainte Catherine, Avignon: H. Dreyfus; Hôpital Saint Jacques, Besançon: M-A. Collonge-Rame; Institut Bergonié, Bordeaux: M.Longy, A. Floquet, E. Barouk-Simonet; CHU, Brest: S. Audebert; Centre François Baclesse, Caen: P. Berthet; Hôpital Dieu, Chambéry: S. Fert-Ferrer; Centre Jean Perrin, Clermont-Ferrand: Y-J. Bignon; Hôpital Pasteur, Colmar: J-M. Limacher; Hôpital d'Enfants CHU – Centre Georges François Leclerc, Dijon: L. Faivre-Olivier; CHU, Fort de France: O. Bera; CHU Albert Michallon, Grenoble: D. Leroux; Hôpital Flaubert, Le Havre: V. Layet; Centre Oscar Lambret, Lille: P. Vennin, C. Adenis; Hôpital Jeanne de Flandre, Lille: S. Lejeune-Dumoulin, S. Manouvier-Hanu; CHRU Dupuytren, Limoges: L. Venat-Bouvet; Centre Léon Bérard, Lyon: C. Lasset, V. Bonadona; Hôpital Edouard Herriot, Lyon: S. Giraud; Institut Paoli-Calmettes, Marseille: F. Eisinger, L. Huiart; Centre Val d'Aurelle

908  
909  
910  
911  
912  
913  
914  
915  
916  
917  
918  
919

– Paul Lamarque, Montpellier: I. Coupier; CHU Arnaud de Villeneuve, Montpellier: I. Coupier, P. Pujol; Centre René Gauducheau, Nantes: C. Delnatte; Centre Catherine de Sienne, Nantes: A. Lortholary; Centre Antoine Lacassagne, Nice: M. Frénay, V. Mari; Hôpital Caremeau, Nîmes: J. Chiesa; Réseau Oncogénétique Poitou Charente, Niort: P. Gesta; Institut Curie, Paris: D. Stoppa-Lyonnet, M. Gauthier-Villars, B. Buecher, A. de Pauw, C. Abadie, M. Belotti; Hôpital Saint-Louis, Paris: O. Cohen-Haguenauer; Centre Viggo-Petersen, Paris: F. Cornélis; Hôpital Tenon, Paris: A. Fajac; GH Pitié Salpêtrière et Hôpital Beaujon, Paris: C. Colas, F. Soubrier, P. Hammel, A. Fajac; Institut Jean Godinot, Reims: C. Penet, T. D. Nguyen; Polyclinique Courlancy, Reims: L. Demange*, C. Penet; Centre Eugène Marquis, Rennes: C. Dugast*; Centre Henri Becquerel, Rouen: A. Chevrier, T. Frebourg, J. Tinat, I. Tennevet, A. Rossi; Hôpital René Huguenin/Institut Curie, Saint Cloud: C. Noguès, L. Demange*, E. Mouret-Fourme; CHU, Saint-Etienne: F. Prieur; Centre Paul Strauss, Strasbourg: J-P. Fricker, H. Schuster; Hôpital Civil, Strasbourg: O. Caron, C. Maugard; Institut Claudius Regaud, Toulouse: L. Gladieff, V. Feillel; Hôpital Bretonneau, Tours: I. Mortemousque; Centre Alexis Vautrin, Vandoeuvre-les-Nancy: E. Luporsi; Hôpital de Bravois, Vandoeuvre-les-Nancy: P. Jonveaux; Gustave Roussy, Villejuif: A. Chompret*, O. Caron). *Deceased prematurely	920 921 922 923 924 925 926 927 928 929 930 931 932 933 934 935 936 937
---	--

## Author contributions

<b>Conceptualization</b> Héctor Climente-González, Christine Lonjou, Chloé-Agathe Azencott.	938 939 940
<b>Data curation</b> Christine Lonjou, GENESIS Study collaborators.	941
<b>Formal Analysis</b> Héctor Climente-González, Christine Lonjou.	942
<b>Funding acquisition</b> Dominique Stoppa-Lyonnet, Nadine Andrieu, Chloé-Agathe Azencott.	943 944
<b>Investigation</b> Héctor Climente-González, Christine Lonjou.	945
<b>Methodology</b> Héctor Climente-González, Christine Lonjou, Chloé-Agathe Azencott.	946
<b>Project administration</b> Chloé-Agathe Azencott.	947
<b>Resources</b> GENESIS Study collaborators, Dominique Stoppa-Lyonnet, Nadine Andrieu.	948 949
<b>Software</b> Héctor Climente-González, Christine Lonjou.	950
<b>Supervision</b> Christine Lonjou, Fabienne Lesueur, Nadine Andrieu, Chloé-Agathe Azencott.	951 952
<b>Validation</b> Christine Lonjou, Fabienne Lesueur.	953
<b>Visualization</b> Héctor Climente-González.	954
<b>Writing – original draft</b> Héctor Climente-González.	955
<b>Writing – review &amp; editing</b> Héctor Climente-González, Christine Lonjou, Fabienne Lesueur, Nadine Andrieu, Chloé-Agathe Azencott.	956 957

## References

1. Bush WS, Moore JH. Chapter 11: Genome-Wide Association Studies. PLoS Computational Biology. 2012;8(12):e1002822. doi:10.1371/journal.pcbi.1002822.
2. Buniello A, MacArthur JA, Cerezo M, Harris LW, Hayhurst J, Malangone C, et al. The NHGRI-EBI GWAS Catalog of published genome-wide association studies, targeted arrays and summary statistics 2019. Nucleic Acids Research. 2019;47(D1):D1005–D1012. doi:10.1093/nar/gky1120.
3. Visscher PM, Wray NR, Zhang Q, Sklar P, McCarthy MI, Brown MA, et al. 10 Years of GWAS Discovery: Biology, Function, and Translation. The American Journal of Human Genetics. 2017;101(1):5–22. doi:10.1016/j.ajhg.2017.06.005.
4. Wang MH, Cordell HJ, Van Steen K. Statistical methods for genome-wide association studies. Seminars in Cancer Biology. 2018;doi:10.1016/j.semcan.2018.04.008.
5. Barton NH, Etheridge AM, Véber A. The infinitesimal model: Definition, derivation, and implications. Theoretical Population Biology. 2017;118:50–73. doi:10.1016/j.tpb.2017.06.001.
6. Boyle EA, Li YI, Pritchard JK. An Expanded View of Complex Traits: From Polygenic to Omnipgenic. Cell. 2017;169(7):1177–1186. doi:10.1016/j.cell.2017.05.038.
7. Furlong LI. Human diseases through the lens of network biology. Trends in Genetics. 2013;29(3):150–159. doi:10.1016/j.tig.2012.11.004.
8. Barabási AL, Gulbahce N, Loscalzo J. Network medicine: a network-based approach to human disease. Nature Reviews Genetics. 2011;12(1):56–68. doi:10.1038/nrg2918.
9. Piñero J, Berenstein A, Gonzalez-Perez A, Chernomoretz A, Furlong LI. Uncovering disease mechanisms through network biology in the era of Next Generation Sequencing. Scientific Reports. 2016;6(1):24570. doi:10.1038/srep24570.
10. Huang JK, Carlin DE, Yu MK, Zhang W, Kreisberg JF, Tamayo P, et al. Systematic Evaluation of Molecular Networks for Discovery of Disease Genes. Cell Systems. 2018;6(4):484–495.e5. doi:10.1016/j.cels.2018.03.001.
11. Azencott CA. Network-Guided Biomarker Discovery. In: Machine Learning for Health Informatics. vol. 9605. Cham: Springer International Publishing; 2016. p. 319–336. Available from: [http://link.springer.com/10.1007/978-3-319-50478-0\\_16](http://link.springer.com/10.1007/978-3-319-50478-0_16).
12. Gwinner F, Boulday G, Vandiedonck C, Arnould M, Cardoso C, Nikolayeva I, et al. Network-based analysis of omics data: The LEAN method. Bioinformatics. 2016; p. btw676. doi:10.1093/bioinformatics/btw676.
13. Jia P, Zheng S, Long J, Zheng W, Zhao Z. dmGWAS: dense module searching for genome-wide association studies in protein–protein interaction networks. Bioinformatics. 2011;27(1):95–102. doi:10.1093/bioinformatics/btq615.

14. Dittrich MT, Klau GW, Rosenwald A, Dandekar T, Muller T. Identifying functional modules in protein-protein interaction networks: an integrated exact approach. *Bioinformatics*. 2008;24(13):i223–i231. doi:10.1093/bioinformatics/btn161.
15. Leiserson MDM, Vandin F, Wu HT, Dobson JR, Eldridge JV, Thomas JL, et al. Pan-cancer network analysis identifies combinations of rare somatic mutations across pathways and protein complexes. *Nature Genetics*. 2015;47(2):106–114. doi:10.1038/ng.3168.
16. Azencott CA, Grimm D, Sugiyama M, Kawahara Y, Borgwardt KM. Efficient network-guided multi-locus association mapping with graph cuts. *Bioinformatics*. 2013;29(13):i171–i179. doi:10.1093/bioinformatics/btt238.
17. Liu Y, Brossard M, Roqueiro D, Margaritte-Jeannin P, Sarnowski C, Bouzigon E, et al. SigMod: an exact and efficient method to identify a strongly interconnected disease-associated module in a gene network. *Bioinformatics*. 2017; p. btx004. doi:10.1093/bioinformatics/btx004.
18. Sinilnikova OM, Dondon MG, Eon-Marchais S, Damiola F, Barjhoux L, Marcou M, et al. GENESIS: a French national resource to study the missing heritability of breast cancer. *BMC Cancer*. 2016;16(1):13. doi:10.1186/s12885-015-2028-9.
19. Michailidou K, Lindström S, Dennis J, Beesley J, Hui S, Kar S, et al. Association analysis identifies 65 new breast cancer risk loci. *Nature*. 2017;551(7678):92–94. doi:10.1038/nature24284.
20. Mulligan AM, , Couch FJ, Barrowdale D, Domchek SM, Eccles D, et al. Common breast cancer susceptibility alleles are associated with tumour subtypes in BRCA1 and BRCA2 mutation carriers: results from the Consortium of Investigators of Modifiers of BRCA1/2. *Breast Cancer Research*. 2011;13(6). doi:10.1186/bcr3052.
21. Rinella ES, Shao Y, Yackowski L, Pramanik S, Oratz R, Schnabel F, et al. Genetic variants associated with breast cancer risk for Ashkenazi Jewish women with strong family histories but no identifiable BRCA1/2 mutation. *Human Genetics*. 2013;132(5):523–536. doi:10.1007/s00439-013-1269-4.
22. Brisbin AG, Asmann YW, Song H, Tsai YY, Aakre JA, Yang P, et al. Meta-analysis of 8q24 for seven cancers reveals a locus between NOV and ENPP2 associated with cancer development. *BMC Medical Genetics*. 2011;12(1):156. doi:10.1186/1471-2350-12-156.
23. SEARCH, The GENICA Consortium, kConFab, Australian Ovarian Cancer Study Group, Ahmed S, Thomas G, et al. Newly discovered breast cancer susceptibility loci on 3p24 and 17q23.2. *Nature Genetics*. 2009;41(5):585–590. doi:10.1038/ng.354.
24. Nielsen FC, van Overeem Hansen T, Sørensen CS. Hereditary breast and ovarian cancer: new genes in confined pathways. *Nature Reviews Cancer*. 2016;16(9):599–612. doi:10.1038/nrc.2016.72.
25. Quigley DA, Fiorito E, Nord S, Van Loo P, Alnaes GG, Fleischer T, et al. The 5p12 breast cancer susceptibility locus affects MRPS30 expression in estrogen-receptor positive tumors. *Molecular Oncology*. 2014;8(2):273–284. doi:10.1016/j.molonc.2013.11.008.

26. Yu M, Li R, Zhang J. Repositioning of antibiotic levofloxacin as a mitochondrial biogenesis inhibitor to target breast cancer. *Biochemical and Biophysical Research Communications*. 2016;471(4):639–645. doi:10.1016/j.bbrc.2016.02.072.
27. Liu G, Claret FX, Zhou F, Pan Y. Jab1/COPS5 as a Novel Biomarker for Diagnosis, Prognosis, Therapy Prediction and Therapeutic Tools for Human Cancer. *Frontiers in Pharmacology*. 2018;9:135. doi:10.3389/fphar.2018.00135.
28. de los Campos G, Vazquez AI, Hsu S, Lello L. Complex-Trait Prediction in the Era of Big Data. *Trends in Genetics*. 2018;34(10):746–754. doi:10.1016/j.tig.2018.07.004.
29. Nikolayeva I, Guitart Pla O, Schwikowski B. Network module identification—A widespread theoretical bias and best practices. *Methods*. 2018;132:19–25. doi:10.1016/j.ymeth.2017.08.008.
30. Ioachim E, Charchanti A, Briassoulis E, Karavasilis V, Tsanou H, Arvanitis DL, et al. Immunohistochemical expression of extracellular matrix components tenascin, fibronectin, collagen type IV and laminin in breast cancer: their prognostic value and role in tumour invasion and progression. *European Journal of Cancer*. 2002;38(18):2362–2370. doi:10.1016/s0959-8049(02)00210-1.
31. Yi W, Xiao E, Ding R, Luo P, Yang Y. High expression of fibronectin is associated with poor prognosis, cell proliferation and malignancy via the NF- $\kappa$ B/p53-apoptosis signaling pathway in colorectal cancer. *Oncology Reports*. 2016;36(6):3145–3153. doi:10.3892/or.2016.5177.
32. Sponzillo M, Rosignolo F, Celano M, Maggisano V, Pecce V, Rose RFD, et al. Fibronectin-1 expression is increased in aggressive thyroid cancer and favors the migration and invasion of cancer cells. *Molecular and Cellular Endocrinology*. 2016;431:123–132. doi:10.1016/j.mce.2016.05.007.
33. Ahmed S, Thomas G, Ghousaini M, Healey CS, Humphreys MK, Platte R, et al. Newly discovered breast cancer susceptibility loci on 3p24 and 17q23.2. *Nature Genetics*. 2009;41(5):585–590. doi:10.1038/ng.354.
34. Breyer J, Dorset D, Clark T, Bradley K, Wahlfors T, McReynolds K, et al. An Expressed Retrogene of the Master Embryonic Stem Cell Gene POU5F1 Is Associated with Prostate Cancer Susceptibility. *The American Journal of Human Genetics*. 2014;94(3):395–404. doi:10.1016/j.ajhg.2014.01.019.
35. Chen HY, Chen RH. Cullin 3 Ubiquitin Ligases in Cancer Biology: Functions and Therapeutic Implications. *Frontiers in Oncology*. 2016;6. doi:10.3389/fonc.2016.00113.
36. Loignon M, Miao W, Hu L, Bier A, Bismar TA, Scrivens PJ, et al. Cul3 overexpression depletes Nrf2 in breast cancer and is associated with sensitivity to carcinogens, to oxidative stress, and to chemotherapy. *Molecular Cancer Therapeutics*. 2009;8(8):2432–2440. doi:10.1158/1535-7163.mct-08-1186.
37. Halsey LG, Curran-Everett D, Vowler SL, Drummond GB. The fickle P value generates irreproducible results. *Nature Methods*. 2015;12(3):179–185. doi:10.1038/nmeth.3288.
38. Wagner A, Wright J. Alternative routes and mutational robustness in complex regulatory networks. *Biosystems*. 2007;88(1-2):163–172. doi:10.1016/j.biosystems.2006.06.002.

39. Gallagher MD, Chen-Plotkin AS. The Post-GWAS Era: From Association to Function. *The American Journal of Human Genetics*. 2018;102(5):717–730. doi:10.1016/j.ajhg.2018.04.002.
40. Cai JJ, Borenstein E, Petrov DA. Broker Genes in Human Disease. *Genome Biology and Evolution*. 2010;2:815–825. doi:10.1093/gbe/evq064.
41. Das J, Yu H. HINT: High-quality protein interactomes and their applications in understanding human disease. *BMC Systems Biology*. 2012;6(1):92. doi:10.1186/1752-0509-6-92.
42. Mishra A, Macgregor S. VEGAS2: Software for More Flexible Gene-Based Testing. *Twin Research and Human Genetics*. 2015;18(1):86–91. doi:10.1017/thg.2014.79.
43. Nakka P, Raphael BJ, Ramachandran S. Gene and Network Analysis of Common Variants Reveals Novel Associations in Multiple Complex Diseases. *Genetics*. 2016;204(2):783–798. doi:10.1534/genetics.116.188391.
44. Ionita-Laza I, Lee S, Makarov V, Buxbaum J, Lin X. Sequence Kernel Association Tests for the Combined Effect of Rare and Common Variants. *The American Journal of Human Genetics*. 2013;92(6):841–853. doi:10.1016/j.ajhg.2013.04.015.
45. Wang M, Huang J, Liu Y, Ma L, Potash JB, Han S. COMBAT: A Combined Association Test for Genes Using Summary Statistics. *Genetics*. 2017;207(3):883–891. doi:10.1534/genetics.117.300257.
46. Xie T. Analysis of the Gene-Dense Major Histocompatibility Complex Class III Region and Its Comparison to Mouse. *Genome Research*. 2003;13(12):2621–2636. doi:10.1101/gr.1736803.
47. Di Tommaso P, Chatzou M, Floden EW, Barja PP, Palumbo E, Notredame C. Nextflow enables reproducible computational workflows. *Nature Biotechnology*. 2017;35(4):316–319. doi:10.1038/nbt.3820.
48. Sakoda LC, Jorgenson E, Witte JS. Turning of COGS moves forward findings for hormonally mediated cancers. *Nature Genetics*. 2013;45(4):345–348. doi:10.1038/ng.2587.
49. Chang CC, Chow CC, Tellier LC, Vattikuti S, Purcell SM, Lee JJ. Second-generation PLINK: rising to the challenge of larger and richer datasets. *GigaScience*. 2015;4(1):7. doi:10.1186/s13742-015-0047-8.
50. Frankish A, Diekhans M, Ferreira AM, Johnson R, Jungreis I, Loveland J, et al. GENCODE reference annotation for the human and mouse genomes. *Nucleic Acids Research*. 2019;47(D1):D766–D773. doi:10.1093/nar/gky955.
51. Wang Q, Jia P. dmGWAS 3.0; 2014. <https://bioinfo.uth.edu/dmGWAS/>.
52. Ljubić I, Weiskircher R, Pferschy U, Klau GW, Mutzel P, Fischetti M. An Algorithmic Framework for the Exact Solution of the Prize-Collecting Steiner Tree Problem. *Mathematical Programming*. 2006;105(2-3):427–449. doi:10.1007/s10107-005-0660-x.
53. Beisser D, Klau GW, Dandekar T, Muller T, Dittrich MT. BioNet: an R-Package for the functional analysis of biological networks. *Bioinformatics*. 2010;26(8):1129–1130. doi:10.1093/bioinformatics/btq089.

54. Dittrich M, Beisser D. BioNet; 2008. <https://bioconductor.org/packages/BioNet/>.
55. Scheid S, Spang R. twilight; a Bioconductor package for estimating the local false discovery rate. *Bioinformatics*. 2005;21(12):2921–2922. doi:10.1093/bioinformatics/bti436.
56. Leiserson MDM, Vandin F, Wu HT, Dobson JR, Eldridge JV, Thomas JL, et al.. HotNet2; 2018. <https://github.com/raphael-group/hotnet2>.
57. Gwinner F. LEANR; 2016. <https://cran.r-project.org/web/packages/LEANR/>.
58. Clemente-González H, Azencott CA. martini; 2019. <https://www.bioconductor.org/packages/martini/>.
59. Liu Y. SigMod v2; 2018. <https://github.com/YuanlongLiu/SigMod>.
60. Jassal B, Matthews L, Viteri G, Gong C, Lorente P, Fabregat A, et al. The reactome pathway knowledgebase. *Nucleic Acids Research*. 2019;doi:10.1093/nar/gkz1031.
61. Yu G, He QY. ReactomePA: an R/Bioconductor package for reactome pathway analysis and visualization. *Molecular BioSystems*. 2016;12(2):477–479. doi:10.1039/c5mb00663e.
62. Benjamini Y, Hochberg Y. Controlling the False Discovery Rate: A Practical and Powerful Approach to Multiple Testing. *Journal of the Royal Statistical Society: Series B (Methodological)*. 1995;57(1):289–300. doi:10.1111/j.2517-6161.1995.tb02031.x.
63. Nogueira S, Brown G. Measuring the Stability of Feature Selection. In: Machine Learning and Knowledge Discovery in Databases. vol. 9852. Cham: Springer International Publishing; 2016. p. 442–457. Available from: [http://link.springer.com/10.1007/978-3-319-46227-1\\_28](http://link.springer.com/10.1007/978-3-319-46227-1_28).
64. Metcalfe KA, Finch A, Poll A, Horsman D, Kim-Sing C, Scott J, et al. Breast cancer risks in women with a family history of breast or ovarian cancer who have tested negative for a BRCA1 or BRCA2 mutation. *British Journal of Cancer*. 2008;100(2):421–425. doi:10.1038/sj.bjc.6604830.
65. Piñero J, Bravo A, Queralt-Rosinach N, Gutiérrez-Sacristán A, Deu-Pons J, Centeno E, et al. DisGeNET: a comprehensive platform integrating information on human disease-associated genes and variants. *Nucleic Acids Research*. 2017;45(D1):D833–D839. doi:10.1093/nar/gkw943.
66. The 1000 Genomes Project Consortium, Gibbs RA, Boerwinkle E, Doddapaneni H, Han Y, Korchina V, et al. A global reference for human genetic variation. *Nature*. 2015;526(7571):68–74. doi:10.1038/nature15393.